Published in final edited form as:

Adv Exp Med Biol. 2012 ; 726: 441–465. doi:10.1007/978-1-4614-0980-9_20.

Assembly and Architecture of HIV

Barbie K. Ganser-Pornillos[1], **Mark Yeager**[1,2], **Owen Pornillos**[1]

[1]Department of Molecular Physiology and Biological Physics, University of Virginia School of Medicine, P.O. Box 800736, Charlottesville, VA 22908, USA

[2]Department of Cell Biology, The Scripps Research Institute, 10550 North Torrey Pines Road, La Jolla, CA 92037, USA

Abstract

HIV forms spherical, membrane-enveloped, pleomorphic virions, 1,000–1,500 Å in diameter, which contain two copies of its single-stranded, positive-sense RNA genome. Virus particles initially bud from host cells in a noninfectious or immature form, in which the genome is further encapsulated inside a spherical protein shell composed of around 2,500 copies of the virally encoded Gag polyprotein. The Gag molecules are radially arranged, adherent to the inner leaflet of the viral membrane, and closely associated as a hexagonal, paracrystalline lattice. Gag comprises three major structural domains called MA, CA, and NC. For immature virions to become infectious, they must undergo a maturation process that is initiated by proteolytic processing of Gag by the viral protease. The new Gag-derived proteins undergo dramatic rearrangements to form the mature virus. The mature MA protein forms a “matrix” layer and remains attached to the viral envelope, NC condenses with the genome, and approximately 1,500 copies of CA assemble into a new cone-shaped protein shell, called the mature capsid, which surrounds the genomic ribonucleoprotein complex. The HIV capsid conforms to the mathematical principles of a fullerene shell, in which the CA sub-units form about 250 CA hexamers arrayed on a variably curved hexagonal lattice, which is closed by incorporation of exactly 12 pentamers, seven pentamers at the wide end and five at the narrow end of the cone. This chapter describes our current understanding of HIV’s virion architecture and its dynamic transformations: the process of virion assembly as orchestrated by Gag, the architecture of the immature virion, the virus maturation process, and the structure of the mature capsid.

1. Introduction

The *Orthoretrovirinae* (orthoretroviruses) comprise the largest subfamily of *Retroviridae* and are subdivided into six genera (alpha, beta, gamma, delta, epsilon, and lentivirus). Orthoretroviruses are spherical membrane-enveloped viruses that bud from the plasma membrane of infected host cells (Fig. 1). The emergent virion is noninfectious, and is characterized by a protein shell located immediately beneath the envelope, which is composed of precursor Gag proteins bound to the inner bilayer leaflet of the viral membrane. During maturation, Gag is cleaved by the viral protease into three new proteins,

Correspondence bpornillos@virginia.edu; yeager@virginia.edu; opornillos@virginia.edu.

called MA, CA, and NC. This disassembles the immature Gag shell and induces structural rearrangements that culminate in formation of the mature, infectious virion. The new MA proteins remain associated with the viral membrane, forming the matrix layer; a subset of the CA proteins assembles into a smaller, mature capsid; and NC condenses with the viral RNA and its associated enzymes into a compact ribonucleoprotein complex within the new capsid. The mature capsid and its contents are called the core.

To initiate replication, the core is introduced into the cytoplasm of a new host cell after receptor binding and fusion of the viral and cellular membranes. The capsid then undergoes a well-ordered but poorly understood uncoating process that culminates in a large enzymatic complex (the “preintegration complex”), which reverse transcribes the RNA genome into a doublestranded DNA copy called the provirus, and then integrates the provirus into the host’s chromosomes. Once integrated, the provirus is transcribed by cellular machinery into various spliced and unspliced mRNA transcripts, which are then translated into the structural and enzymatic viral proteins required to maintain infection and propagate new virions.

Orthoretroviruses include important human pathogens (e.g., HTLV-1 and HTLV-2, which cause T-cell leukemias). The most significant of these has been HIV-1, which causes exceptionally high mortality rates through AIDS. The number of people living with HIV is currently estimated to be in excess of 33 million, with 2.7 million new infections and 2 million AIDS-related deaths in 2008 (UNAIDS 2009). HIV-1 is, therefore, one of the most studied viruses and is discussed here as a model system for other orthoretroviruses. It is important to note, however, that valuable assembly principles have been discovered through studies of other orthoretroviruses (e.g., RSV, MLV). Furthermore, although the general principles of orthoretroviral structure and assembly are conserved, virus-specific variations also exist. The virus-specific features presumably reflect unique selective pressures or adaptations between a particular virus and its host.

2. Assembly and Architecture of the Immature Virion

Assembly of the immature virion is orchestrated by the precursor Gag protein (Fig. 2a). In fact, all the information necessary for assembly of a retrovirus is encoded in Gag. For instance, recombinant expression of Gag in the absence of all other viral proteins results in efficient release of immature particles (Gheysen et al. 1989). In addition, pure recombinant Gag proteins can assemble *in vitro* into spherical shells that resemble immature virions (Campbell and Vogt 1997; Campbell and Rein 1999; Gross et al. 2000; Campbell et al. 2001).

Gag is organized as a series of functional “modules” that work in concert to: (1) target Gag molecules to assembly sites at the plasma membrane, (2) create a membrane-bound protein shell composed of Gag hexamers, (3) specifically recognize and encapsulate the dimeric viral genome, (4) recruit and incorporate all other virus components into the assembling particle, and (5) conscript the required cellular factors and chaperones, such as the ESCRT budding machinery. The HIV-1 Gag protein is composed of four independently folded structural domains that are demarcated by flexible regions (Fig. 2a). The N-terminal domain corresponds to the mature MA protein, which is cotranslationally modified with a fatty acid

chain (myristic acid) and facilitates Gag binding to the viral envelope. The MA domain (colored red in Fig. 2a) targets Gag to assembly sites at the plasma membrane and facilitates incorporation of the envelope glycoproteins into the assembling virion. The two central domains of Gag correspond to the mature CA protein, which is formed by independently folded N-terminal and C-terminal domains, which we designate as CA^{NTD} and CA^{CTD} (colored green and cyan in Fig. 2a). These domains mediate the principal Gag–Gag contacts in both the immature Gag shell and the mature capsid. The fourth domain corresponds to the mature NC protein and, in HIV-1, is composed of two zinc fingers (colored blue in Fig. 2a) that bind the RNA genome. High-affinity NC–RNA interactions enable specific recognition and packaging of two copies of the genome, whereas low-affinity interactions promote Gag assembly. HIV-1 Gag contains an additional region at its C terminus, called p6, which is specific to lentiviruses. The p6 sequence lacks a defined tertiary structure, but contains two peptide motifs (called “late domains”) that function as docking sites for the cellular ESCRT machinery, which facilitates the release of newly assembled virions from the cell surface. (Other orthoretroviral Gag proteins harbor late domains with equivalent functions, but at different positions in the Gag primary sequence.) HIV-1 Gag also contains two spacer peptides, called SP1 and SP2, which respectively demarcate the CA/NC and NC/p6 domains. SP1 is a critical maturation switch, and equivalent regions are found in other orthoretroviruses.

Retrovirus assembly appears to be initiated by just a few Gag molecules that are specifically bound to two copies of the RNA genome (Jouvenet et al. 2009; Miyazaki et al. 2010). The molecular mechanism by which HIV-1 Gag specifically recognizes its genome is not yet fully elucidated, but studies of Moloney murine leukemia virus have identified an RNA switch that couples genomic dimerization and packaging (D’Souza et al. 2001; D’Souza and Summers 2004; Dey et al. 2005; Gherghe et al. 2010). Conserved sequence elements in the genomic packaging signal (called Ψ) are sequestered by intramolecular base pairing in the monomeric RNA and then become exposed upon dimerization, thereby allowing specific, high-affinity binding of the RNA dimer to the NC domain (D’Souza and Summers 2004). Upon nucleation, stochastic addition of Gag molecules extends the assembling lattice and curves the membrane outward, culminating in an immature particle whose envelope remains connected to the cellular plasma membrane by a narrow stalk. Live-cell imaging studies show that Gag proteins accumulate fairly rapidly at the membrane assembly site, and the immature shell is essentially complete about 10 min after nucleation (Jouvenet et al. 2008; Ivanchenko et al. 2009). However, the newly formed virion does not bud for another 15 min, suggesting that fission of the membrane stalk may be a rate-limiting step in virion formation (Ivanchenko et al. 2009).

2.1 Functions of the Gag MA Domain

The MA domain of HIV-1 Gag adopts a helical tertiary fold (Massiah et al. 1994; Hill et al. 1996), harbors the myristyl fatty acid modification at its N terminus (Göttlinger et al. 1989), directly mediates contacts between Gag and the plasma membrane (Spearman et al. 1994; Zhou et al. 1994), and facilitates incorporation of the envelope proteins into the assembling virion (Yu et al. 1992; Dorfman et al. 1994; Freed and Martin 1995, 1996) (Fig. 3).

Membrane Binding and Targeting.—Low-angle X-ray solution scattering studies indicate that newly translated HIV-1 Gag proteins adopt a “folded-over” conformation, wherein the MA and NC domains are in proximity (Datta et al. 2007a) (Fig. 3a). In this soluble conformation, the N-terminal myristyl group (colored green in Fig. 3a) is sequestered in a hydrophobic pocket in MA (Tang et al. 2004), which would presumably disfavor membrane binding. Stable attachment to the membrane requires three synergistic elements: (1) exposure of the myristyl group, (2) binding of the MA domain through nonspecific electrostatic interactions with negatively charged phospholipid headgroups and specific interactions with phosphatidylinositol-4,5-bisphosphate [PI(4,5)P_2], and (3) Gag oligomerization, wherein Gag adopts an extended conformation and begins to assemble into the immature shell (Zhou et al. 1994; Spearman et al. 1997; Paillart and Göttlinger 1999; Ono et al. 2000, 2004; Tang et al. 2004; Dalton et al. 2005, 2007; Saad et al. 2006; Datta et al. 2007b; Li et al. 2007). PI(4,5)P_2 (colored yellow in Fig. 3a) is enriched in the plasma membrane, and depletion of the cellular pools of this phosphoinositide incorrectly directs HIV-1 Gag to internal membranes (Ono et al. 2004). Thus, PI(4,5)P_2 binding simultaneously promotes stable membrane binding and proper targeting of Gag molecules to assembly sites at the plasma membrane.

The molecular mechanism by which PI(4,5)P_2 binding and myristyl exposure are coupled is now understood in detail (Saad et al. 2006) (Fig. 3). PI(4,5)P_2 belongs to a large class of membrane bilayer lipids (phosphatidylinositols), which are composed of a glycerol backbone, one saturated and one unsaturated fatty acid chain (which are attached to the 1’ and 2’ positions of the glycerol backbone, respectively), and a phosphoinositol headgroup (attached to the 3’ glycerol position). The phosphoinositol headgroup binds to a basic patch on the surface of MA and confers binding specificity. The 2’ unsaturated fatty acid chain is extruded from the lipid bilayer and binds in a hydrophobic groove adjacent to the myristyl binding groove. The 1’ saturated fatty acid chain does not interact with MA, but rather anchors Gag to the membrane. PI(4,5)P_2 and myristyl binding to the globular MA domain are mutually exclusive: upon binding, PI(4,5)P_2 repositions hydrophobic residues in the myristyl binding pocket, triggering exposure of the myristyl group. The exposed myristyl fatty acid chain then inserts into the lipid bilayer, forming a second membrane anchor.

It is intriguing that membrane-bound Gag proteins are anchored by two fully saturated fatty acid chains (Saad et al. 2006). This has been suggested as a potential mechanism for partitioning membrane-bound Gag into lipid microdomains (e.g., so-called lipid rafts) because rafts preferentially interact with saturated fatty acid chains (Brown and London 1997; Zacharias et al. 2002). Live-cell fluorescence imaging studies support this idea and show that Gag assembles at punctate sites at the plasma membrane (Hermida-Matsumoto and Resh 2000; Jouvenet et al. 2008; Ivanchenko et al. 2009), which appear to correspond to lipid microdomains (Aloia et al. 1993; Nguyen and Hildreth 2000; Ono and Freed 2001; Brügger et al. 2006).

Recruitment and Incorporation of Envelope Proteins.—The exterior of HIV-1 virions is studded with trimeric envelope (Env) glycoprotein spikes composed of an ectodomain (gp120) and a transmembrane domain (gp41). The Env proteins mediate receptor-mediated fusion of viral and cellular membranes to initiate infection. The Env

proteins are translated by ER-associated ribosomes as a single precursor polypeptide, called gp160, which is transported to the plasma membrane via the cellular secretory pathway. During transport, gp160 is extensively glycosylated, associates into trimers, and is cleaved by the cellular protease furin into the mature subunits (Swanstrom and Wills 1997). Incorporation of the Env proteins into the assembling virion is thought to be mediated by interactions between the MA domain and the cytoplasmic tail of gp41 (Yu et al. 1992; Dorfman et al. 1994; Freed and Martin 1995, 1996; Murakami and Freed 2000a), which may occur through a bridging cellular protein (Lopez-Vergès et al. 2006). Passive incorporation of Env may also occur through simple mass action (Murakami and Freed 2000b).

2.2 Gag–Gag Lattice Interactions

The immature virion contains around 2,500 copies of the Gag protein (Carlson et al. 2008), which assemble into a spherical shell immediately beneath the viral envelope. The assembled Gag molecules adopt an extended “beads on a string” configuration, wherein the sequential domains are arranged with the Gag N terminus on the outermost edge of the shell, and the C terminus points toward the center of the virion (Fuller et al. 1997; Yeager et al. 1998) (Fig. 2b). As discussed in the above section, the N terminus of Gag is tethered to the membrane by the MA domain. Although MA by itself can form trimers (Hill et al. 1996; Tang et al. 2004) (Fig. 3b), it does not form an extended lattice in the immature virion (Wright et al. 2007; Carlson et al. 2008; Briggs et al. 2009; de Marco et al. 2010; Keller et al. 2011) and is dispensable for particle assembly (Wang et al. 1993; Reil et al. 1998; Gross et al. 2000; Briggs et al. 2009). The C-terminal NC domain is also dispensable, provided it is replaced by a heterologous domain that is capable of self-association (e.g., leucine zipper motifs) (Zhang and Barklis 1997). NC itself does not appear to form direct lattice-stabilizing contacts, but contributes to particle formation by tethering Gag to the RNA genome (via nonspecific contacts, as opposed to specific binding to the dimeric Ψ packaging element), thereby increasing the effective concentration of the assembling Gag molecules (Campbell and Vogt 1997; Gross et al. 2000).

The principal sites of lateral Gag–Gag interactions are located in the CA^{NTD} and CA^{CTD} domains, as well as the SP1 linker. These structural elements facilitate Gag assembly by forming a paracrystalline lattice of close-packed hexamers (Fig. 4).

The CA^{NTD} is an arrowhead-shaped domain composed of seven α-helices (numbered 1–7) (Gitti et al. 1996; Tang et al. 2002; Kelly et al. 2006) and directly contributes to Gag assembly by forming hexameric rings (Fig. 2a and Fig. 4). In reconstructed cryotomograms of immature particles, the CA^{NTD} hexamers are about 80 Å in diameter and interact across the threefold and/or twofold axes of the hexagonal lattice (Wright et al. 2007; Briggs et al. 2009; de Marco et al. 2010; Keller et al. 2011) (Fig. 4a, b, green). The current tomograms are not of sufficient resolution to unambiguously define domain orientations. However, biochemical analyses have identified two surfaces of CA^{NTD} that are important for Gag assembly: one encompassing helices 1 and 2, and a second near helices 4 and 7 (von Schwedler et al. 2003 a; Lanman et al. 2004; Mortuza et al. 2008; Monroe et al. 2010). One suggested model is that the sixfold symmetric interactions are mediated by the first region, and interhexamer contacts are mediated by the second (Wright et al. 2007).

The CA^{CTD} is a globular domain composed of a short 3_{10}-helix/strand/α-helix element termed the major homology region (MHR), and four a-helices (numbered 8–11) (Gamble et al. 1997; Worthylake et al. 1999) (Fig. 2a). Cryotomograms indicate that in the immature lattice, CA^{CTD} forms a second layer of hexamers directly below and with a similar (if slightly smaller) spacing as the CA^{NTD} layer (Wright et al. 2007; Briggs et al. 2009; de Marco et al. 2010) (Fig. 4a, b, cyan). The CA^{CTD} hexamers interact across the twofold symmetry axes of the hexagonal lattice, and this is consistent with biochemical data showing that the isolated CA^{CTD} is a dimer in solution (Gamble et al. 1997; Ivanov et al. 2007; Byeon et al. 2009). High-resolution X-ray and NMR structures of the isolated CA^{CTD} dimer have identified at least two dimerization modes (side-by-side and domain-swapped, with at least three possible side-by-side configurations) (Gamble et al. 1997; Worthylake et al. 1999; Ivanov et al. 2007; Bartonova et al. 2008; Byeon et al. 2009). However, the current cryotomograms cannot unambiguously discriminate which of these structures may exist in immature virions.

Cryotomograms of immature particles reveal a third layer of hexagonal order beneath the CA^{CTD} hexamers, which is composed of pillars of density that extend toward the NC/RNA region (Wright et al. 2007; Carlson et al. 2008; Briggs et al. 2009; de Marco et al. 2010; Keller et al. 2011) (Fig. 4a, b, gray). The pillars are interpreted as ordered residues at the CA/SP1 boundary, which is consistent with the finding that this region is essential for assembly of immature HIV-1 particles (Kräusslich et al. 1995; Accola et al. 1998). Residues at the CA/SP1 boundary have been previously predicted to adopt an α-helical secondary structure (Fig. 2a) to mediate quaternary Gag–Gag contacts in the immature shell (Accola et al. 1998; Worthylake et al. 1999; Liang et al. 2002; Newman et al. 2004; Morellet et al. 2005). Although the quaternary arrangement of the putative CA/SP1 helices is not yet firmly established, one proposal is that this region forms a sixfold symmetric helical bundle beneath the CA^{CTD} hexamer (Wright et al. 2007). Analogous regions have been identified in biochemical and structural analyses of other orthoretroviruses (Cheslock et al. 2003; Keller et al. 2008; de Marco et al. 2010), suggesting that structural roles of the CA/SP1 boundary residues are conserved.

Although our understanding of the architecture of the immature Gag shell is at an early stage, it is apparent that inherent curvature of the hexagonal Gag lattice likely arises from a systematic decrease in hexamer-to-hexamer packing distances across the sequential CA^{NTD}, CA^{CTD}, and SP1 (or equivalent) layers (Wright et al. 2007; Briggs et al. 2009) (Fig. 4a). Spherical hexagonal lattices cannot sustain long-range hexagonal order and must incorporate defects in order to maintain similar quaternary contacts across the different subunits. Quasi-equivalent icosahedral viruses and mature orthoretroviral capsids incorporate defects with local fivefold rotational symmetry (typically occupied by pentamers). In a hexagonal lattice, 12 such defects simultaneously accommodate lattice curvature and mediate shell closure. In contrast, the immature Gag lattice does not appear to contain pentamers and instead employs irregular defects of various geometries (Briggs et al. 2009) (Fig. 4c). Furthermore, the Gag shell is not completely closed, and surprisingly large regions (up to 50% of the virion) are devoid of ordered Gag molecules (Wright et al. 2007; Briggs et al. 2009; de Marco et al. 2010; Keller et al. 2011). It is not clear why orthoretroviruses do not form fully closed immature shells. One proposal is that Gag assembly is in kinetic competition with budding,

and that membrane scission and virion release typically occur before complete Gag shells can be assembled (Carlson et al. 2008).

3. Budding

Virion release proceeds through the formation of a constriction in the connecting membrane, which produces both positive and negative curvatures in the lipid bilayer (Fig. 5). Membrane curvature during budding appears to not only be mediated by Gag but also by additional contributions from cellular proteins, and possibly, membrane lipids (Le Blanc et al. 2002; Wang et al. 2003; Carlson et al. 2008). Abscission of the connecting membrane and release of the nascent virion requires membrane fission, which is facilitated by cellular machinery that normally functions in the ESCRT budding pathway (Fig. 5).

The ESCRT pathway comprises protein complexes (called ESCRT-0, ESCRT-I, ESCRT-II, ESCRT-III, and a dodecameric AAA ATPase called VPS4) that cycle between the cytoplasm and late endosomal membranes (Fig. 5a). On the surface of the endosome, ESCRT complexes have at least three functions: (1) sort protein cargos tagged with monoubiquitin into specific areas, (2) induce membrane invagination toward the lumen of the endosome and away from the cytoplasm (which results in formation of vesicles that are connected to the endosomal membrane, analogous to assembled immature virions), and (3) facilitate budding of the vesicles (Hurley and Emr 2006). During cell division, ESCRT complexes also facilitate abscission of the midbody, thereby separating the two daughter cells (Carlton and Martin-Serrano 2007; Morita et al. 2007).

The mammalian ESCRT pathway is quite elaborate, and orthoretroviruses have evolved multiple short peptide motifs called “late domains” that mediate different entry points into the pathway (Fig. 5a). HIV-1 has two well-characterized late domains that are contained in the p6 region of Gag. These comprise the peptide sequences Pro-Thr/Ser-Ala-Pro (PTAP) and Tyr-Pro-X_n-Leu (YPXL), which respectively bind the proteins TSG101 (a component of the ESCRT-I complex) (Garrus et al. 2001; Martin-Serrano et al. 2001; VerPlank et al. 2001; Pornillos et al. 2002) or ALIX (which binds ESCRT-I and ESCRT-III proteins) (Strack et al. 2003; von Schwedler et al. 2003b; Zhai et al. 2008). HIV-1 and other orthoretroviruses also recruit members of the NEDD4 family of ubiquitin ligases, either via Pro-Pro-X-Tyr (PPXY) late domains (Kikonyogo et al. 2001; Yasuda et al. 2002; Bouamr et al. 2003) or via alternative interactions that have yet to be defined precisely (Chung et al. 2008; Usami et al. 2008). These late domain interactions lead to the eventual recruitment and conscription of the core fission machinery [composed of the ESCRT-III complex and the VPS4 enzyme (Wollert et al. 2009)], which then facilitates release of new virions from the cell surface.

One proposed mechanism of membrane fission at the neck of the budding virion has been inferred from the observation that a subset of ESCRT-III proteins (also called CHMPs) self-assemble into tubular structures with dome-like caps, whose external surfaces are lined with positively charged residues and, therefore, have considerable affinity for acidic phospholipid headgroups (Ghazi-Tabatabai et al. 2008; Hanson et al. 2008; Lata et al. 2008; Bajorek et al. 2009). The basic model is that assembly of the dome-like structure within the budding neck creates large elastic stress in the lipid bilayer, which drives membrane fission and separation

of the viral and cellular membranes (Fabrikant et al. 2009) (Fig. 5b). Following release of the virion, the VPS4 enzyme uses energy derived from ATP hydrolysis to disassemble the ESCRT-III dome, and thereby resets the system for another round of membrane fission (Lata et al. 2008; Wollert et al. 2009).

4. Virion Maturation

Maturation transforms the noninfectious immature virion into a particle that is capable of transmitting infection. This process is initiated by proteolytic processing of Gag by the viral protease (PR) (Fig. 6). HIV-1 PR is encoded within the Gag–Pol fusion protein, which arises from a ribosomal frameshift during translation at the 3' end of the *gag* gene (which occurs 5% of the time). The Gag–Pol proteins are packaged into virions through the immature lattice interactions mediated by the Gag region. The enzyme active site is created by PR dimerization, and the functional protease is liberated by autoproteolysis during or immediately after budding (Lapatto et al. 1989; Navia et al. 1989; Kräusslich 1991). Virions arrested at the late budding stage display immature morphology, implying that budding and maturation are intimately coupled events (Göttlinger et al. 1991).

The five proteolysis sites in HIV-1 Gag are cleaved at different rates, in the order: SP1/NC > MA/CA and SP2/p6 > NC/SP2 > CA/SP1 (Pettit et al. 1998) (Fig. 6a). This results in a defined sequential release of maturation intermediates. Mutations that disrupt cleavage of individual sites or alter the processing order result in particles that have severely reduced infectivity, indicating that both the accuracy and timing of Gag processing are essential for proper maturation (Tritch et al. 1991; Wiegers et al. 1998). Furthermore, doping the immature virion with Gag processing intermediates interferes with maturation, implying that individual Gag molecules are not cleaved at random (Müller et al. 2009). This is consistent with the idea that PR processing is initiated at the rim of the ordered Gag lattice in the incompletely closed immature shell and then proceeds as a "wave" into the interior of the lattice (Carlson et al. 2008); Müller et al. 2009).

Gag cleavage by PR disassembles the immature lattice and liberates the subunits of the mature capsid (the CA protein). CA is derived from the central region of the Gag precursor and is the last mature protein to be released as a result of sequential processing of Gag's proteolytic sites (Fig. 6a).

Although a precise understanding of the molecular transformations that occur during maturation must await a high-resolution structure of the immature Gag lattice, deuterium exchange and mutagenesis studies indicate that the two CA domains (CA^{NTD} and CA^{CTD}) utilize highly overlapping interfaces to mediate interactions in both the immature and mature lattices (Lanman et al. 2003, 2004; von Schwedler et al. 2003 a; Monroe et al. 2010). Indeed, the tertiary structures of these two domains are largely preserved in the Gag polyprotein and mature CA, except for residues in the immediate vicinity of the proteolytic sites (Worthylake et al. 1999; Tang et al. 2002; Newman et al. 2004; Kelly et al. 2006) (Fig. 6b).

Proteolytic cleavage at the N-terminal end of CA releases the protein from the upstream MA domain and results in refolding of the first 13 residues of CA from an extended

conformation into a β-hairpin (colored yellow in Fig. 6b). The β-hairpin is stabilized by a salt bridge between the new Pro1 imino group and a conserved acidic residue (Asp51 in HIV-1) (Gitti et al. 1996; von Schwedler et al. 1998). Formation of the β-hairpin probably destabilizes the immature $_{CA}^{NTD}$ hexamer and facilitates proper juxtaposition of the adjacent domains in the mature hexamer conformation (Gross et al. 1998; von Schwedler et al. 1998; Kelly et al. 2006; Pornillos et al. 2010). Interestingly, it appears that folding of the β-hairpin does not proceed immediately after cleavage of the MA/CA junction, but after the final proteolytic processing step at the CA/SP1 junction (Monroe et al. 2010). Thus, cleavage at the CA C terminus appears to be the dominant maturation switch. Indeed, mutagenesis of this region is particularly detrimental to capsid assembly and virus infectivity (Kräusslich et al. 1995; Gross et al. 2000; Li et al. 2003; Müller et al. 2009). Proteolysis of the CA/SP1 junction is expected to unravel the putative helical bundle in this region that helps stabilize the immature lattice, and indeed, the last 11 residues of CA appear to be disordered in the mature capsid (Ganser-Pornillos et al. 2007; Pornillos et al. 2009).

Studies of other orthoretroviruses have revealed comparable structural switches at the CA termini. For example, folding of the β-hairpin during maturation appears to be a general switch because N-terminal extensions shift the *in vitro* assembly phenotypes of HIV-1, RSV, and MPMV CA proteins from mature-like particles to immature-like particles (Campbell and Vogt 1997; Gross et al. 1998; von Schwedler et al. 1998; Rumlova-Klikova et al. 2000). Interestingly, spacer peptides upstream of the CA domains of RSV and MPMV appear to make important protein–protein interactions in the immature lattice that are not present in HIV-1 (Joshi and Vogt 2000; Knejzlík et al. 2007; Phillips et al. 2008). The best-characterized example is the “p10” region immediately upstream of RSV CA, which folds into a helix and packs against the globular CA^{NTD} domain (Nandhagopal et al. 2004). This interaction is important for RSV Gag hexamerization and lattice assembly (Joshi and Vogt 2000; Phillips et al. 2008). Assembly regions downstream of CA, which are analogous to the SP1 spacer in HIV-1, have also been identified in MLV, RSV, and MPMV Gag, even though these proteins lack a bona fide spacer between their CA and NC domains (Cheslock et al. 2003; Keller et al. 2008; de Marco et al. 2010). Indeed, pillar-like densities below the $_{CA}^{CTD}$ hexamer layer are also visible in cryotomographic reconstructions of immature MPMV and RSV particles, although the MPMV pillar appears much smaller than in either HIV-1 or RSV (de Marco et al. 2010). These examples highlight both the degree of conservation in the assembly principles of orthoretroviruses and the structural/mechanistic variations that different viruses use to reach the same endpoint.

5. Assembly and Architecture of the Mature Capsid

In the infectious retrovirion, the ribonucleoprotein genomic complex is contained within the mature capsid, which is composed of around 1,500 copies of the mature CA protein (Fig. 2c). The architecture of the mature capsid of HIV-1 is described by the geometric principles of a fullerene cone (Ganser et al. 1999; Jin et al. 1999; Li et al. 2000; Heymann et al. 2008). The body of the capsid is a cone-shaped two-dimensional lattice of CA hexamers. By analogy to quasi-equivalent icosahedral viruses, the hexagonal capsid lattice incorporates 12 pentamers to form a closed shell. The pentamers are also composed of CA and are

distributed asymmetrically across the capsid shell. Thus, the capsid itself is globally asymmetric even though it is composed of locally symmetric building blocks.

The mature capsids of orthoretroviruses adopt different preferred shapes and are primarily cones in HIV-1 and lentiviruses, cylinders in betaretroviruses (e.g., MPMV), and polyhedral or "spherical" in others (e.g., RSV, MLV) (Vogt 1997). The various shapes are a consequence of the distribution of the pentamers: "spherical" capsids have the 12 pentamers distributed randomly, cylinders have six pentamers at each end of a tube, and cones have five pentamers at the narrow end and seven at the wide end (Fig. 7) (Ganser-Pornillos et al. 2004; Benjamin et al. 2005; Briggs et al. 2006; Butan et al. 2008). This is in stark contrast to icosahedral capsids, wherein the 12 pentamers are arranged in a symmetric configuration.

5.1 CA–CA Lattice Interactions

Electron cryomicroscopy and cryotomography of mature virions and capsids of HIV-1 (Briggs et al. 2003, 2006; Benjamin et al. 2005) and RSV (Butan et al. 2008) confirm the essential tenets of the fullerene model and reveal that the hexamer-to-hexamer spacing in the mature lattice is 90–100 Å (Briggs et al. 2003). The mature CA hexamer is distinct from the immature Gag hexamer, and therefore the intersubunit interactions mediated by CA^{NTD} and CA^{CTD} must rearrange during maturation.

To a large extent, our understanding of the quaternary interactions in the mature capsid is derived from analyses of *in vitro* model systems that are assembled from purified recombinant CA proteins (Ehrlich et al. 1992; Campbell and Vogt 1995; Gross et al. 1997; Kingston et al. 2000; Ganser-Pornillos et al. 2007; Purdy et al. 2008). These assemblies recapitulate the local symmetry of the building blocks but are also globally symmetric and are, thus, more amenable to biochemical and structural analyses (Fig. 8). For example, helical tubes and two-dimensional crystals composed of CA hexamers have provided low-resolution views of the hexagonal lattice (Li et al. 2000; Ganser- Pornillos et al. 2007; Byeon et al. 2009), whereas icosahedral assemblies of RSV CA allowed the first visualization of the CA pentamer (Cardone et al. 2009; Hyun et al. 2010). Biochemical and mutagenesis experiments have established that these *in vitro* assemblies faithfully recapitulate the lattice interactions of CA subunits in mature capsids (Gross et al. 1997; von Schwedler et al. 1998, 2003 a; Lanman et al. 2003; Ganser-Pornillos et al. 2004; Purdy et al. 2008).

The assembly functions of the CA^{NTD} and CA^{CTD} domains in the mature capsid are clearly delineated: CA^{NTD} forms sixfold or fivefold symmetric rings, whereas side-by-side CA^{CTD} dimers connect each ring to its neighbors (Fig. 9, Fig. 10 and Fig. 11). Furthermore, the CA^{CTD} domains form a "belt" surrounding the central CA^{NTD} ring, with each CA^{CTD} packed against the CA^{NTD} of the adjacent subunit (Fig. 9). The quaternary intersubunit interactions in the CA hexamer, pentamer, and dimer have each now been visualized at atomic resolution. Thus, the architecture of the mature capsid is now understood in considerable detail (Fig. 9).

The CA^{NTD} Hexamer and Pentamer.—The CA^{NTD} hexamer is a sixfold symmetric ring that is organized around an 18-helix barrel composed of the first three helices of each subunit (Mortuza et al. 2004; Ganser-Pornillos et al. 2007; Pornillos et al. 2009) (Fig. 9b and

Fig. 10a). The repeating interaction is a three-helix bundle formed by lengthwise packing of helix 2 from one subunit against helices 1 and 3 of the adjacent subunit. In HIV-1, the center of the three-helix bundle contains a small hydrophobic core composed of aliphatic side chains (Fig. 10c), whereas interactions at the periphery are mediated by polar residues. Direct electrostatic protein-protein contacts are conspicuously absent, and essentially all the intersubunit hydrogen bonds are bridged by water molecules (Pornillos et al. 2009).

The quaternary organization of the CA^{NTD} pentamer is similar to the hexamer, except that the subunits form a fivefold symmetric ring organized around a 15-helix barrel (Cardone et al. 2009; Hyun et al. 2010; Pornillos et al. 2011) (Fig. 9c and Fig. 10b). Even though the packing angles between adjacent subunits are different, the HIV-1 pentamer uses a similar three-helix repeat unit – stabilized by essentially identical hydrophobic interactions – as the hexamer (Pornillos et al. 2011) (Fig. 10c).

Switching between the CA^{NTD} hexamer and pentamer follows the general model for quasi-equivalence as originally proposed by Caspar and Klug (1962). Alternative packing of subunits in the two oligomers occurs by a simple rotation of adjacent subunits, about an axis that appears to coincide with the precise center of the three-helix repeat unit (Pornillos et al. 2011) (Fig. 10d). Residues at the center of the three-helix repeat unit can therefore maintain essentially the same hydrophobic packing interactions in both oligomers, and only subtle rearrangements in the hydrogen-bonding interactions at the inner and outer rims of the CA^{NTD} rings are required.

The energetic landscape of hexamer vs pentamer assembly appears to be controlled by an electrostatic switch (Cardone et al. 2009; Pornillos et al. 2011). In the case of HIV-1 CA, an almost universally conserved arginine residue (Arg18) occupies an annulus at the centers of both the hexamer and pentamer. Juxtaposition of like charges creates electrostatic repulsion, which is greater for the pentamer because the arginine residues are closer to each other in the fivefold ring (Pornillos et al. 2011). Indeed, substitution of Arg18 with uncharged residues promotes pentamer formation *in vitro* (Ganser-Pornillos et al. 2004, 2007). Electrostatic destabilization of the pentamer is most probably counterbalanced by local assembly rules and cooperativity, such that a pentamer is integrated into the assembling capsid lattice only at a position where incorporation of a hexamer is incompatible with the local lattice curvature.

The CA^{CTD} Dimer.—The CA^{CTD} hexamers and pentamers are linked into a continuous lattice by symmetric CA^{CTD} dimers (Fig. 11a), with side-by-side interacting subunits (i.e., not domain-swapped). The affinity of the mature HIV-1 CA^{CTD} dimer is measurable in solution, with a dissociation constant (K_d) of ~10^{-5} M (Gamble et al. 1997; Byeon et al. 2009). Characterized CA proteins of other orthoretroviruses remain monomeric in solution (Khorasanizadeh et al. 1999; Campos-Olivas et al. 2000; Mortuza et al. 2009) but also form analogous dimers under conditions that promote capsid assembly (Bailey et al. 2009; Purdy et al. 2009). The CA^{CTD} dimer interface is mediated by symmetric packing of helix 9 across the dyad, and hydrophobic interactions between the 3_{10} helix of one subunit and helix 9 of the other (Gamble et al. 1997; Worthylake et al. 1999; Byeon et al. 2009). The lattice-stabilizing dimer inter-face is the same as the solution dimer interface (Ganser-Pornillos et

al. 2007; Byeon et al. 2009), implying that the basic assembly unit of the mature capsid is composed of two CA subunits linked by CA^{CTD}.

5.2. Mechanisms of Capsid Lattice Curvature

A key feature of the HIV-1 fullerene cone capsid is that the curvature of the hexagonal CA lattice changes continuously (Ganser et al. 1999; Li et al. 2000) (Fig. 11). This is most easily appreciated by considering the bite angle between adjacent hexamers. The bite angles change continuously and range from around 135° between two hexamers connected to the same pentamer at the ends of the cone to around 180° in more flat regions at the body of the cone. The CA protein has the requisite flexibility for creating such a variably curved lattice because the CA^{NTD} and CA^{CTD} domains are linked by a flexible stretch of four amino acid residues. Indeed, NMR analyses of full-length CA proteins in solution demonstrate that the two domains can rotate almost independently of each other (Khorasanizadeh et al. 1999; Campos-Olivas et al. 2000). In the assembled lattice, the relative orientations of the CA^{NTD} rings and CA^{CTD} dimers can also vary (Byeon et al. 2009; Cardone et al. 2009; Pornillos et al. 2009). Unlike the soluble CA protein, however, movement of the two domains in the assembled lattice is more restricted. One proposal is that capsid lattice curvature is mediated by defined modes of flexibility at two assembly interfaces: the NTD-CTD and CTD-CTD interfaces (Pornillos et al. 2011) (Fig. 11).

NTD–CTD Interactions.—In the assembled CA lattice, each CA^{CTD} domain packs against the CA^{NTD} domain from the adjacent subunit, via an intermolecular set of interactions called the NTD–CTD interface (Bowzard et al. 2001; Lanman et al. 2003; Ganser-Pornillos et al. 2007) (Fig. 11b). A critical feature of the NTD–CTD interface is that it contains a set of direct protein–protein hydrogen bonds, each of which is a helix-capping interaction, and connects a flexible polar side chain in one domain with a helix terminus in the other domain (Pornillos et al. 2009, 2011). These helix-capping hydrogen bonds act as molecular pivots for limited rigid-body rotations of CA^{CTD} relative to CA^{NTD} (indicated by red double-headed arrow in Fig. 11b). In this manner, the NTD–CTD interface can restrict the movement of the CA^{CTD} dimers relative to the CA^{NTD} rings. Each dimer can only rotate about a fixed axis that is approximately parallel to the plane of the ring, and this flexion would allow each CA^{NTD} ring to adopt slightly different bite angles relative to its neighbors. The NTD–CTD interface, therefore, is likely to function by channeling the native flexibility of the CA protein into a mechanism for generating variable lattice curvature. This feature is common to the hexamer and pentamer since an identical set of interactions is found in both capsomers (Pornillos et al. 2009, 2011).

CTD–CTD Interactions.—Biochemical and structural analyses also indicate that the CA^{CTD} domain is conformationally flexible (Ternois et al. 2005; Alcaraz et al. 2007; Ganser-Pornillos et al. 2007; Ivanov et al. 2007; Bartonova et al. 2008; Wong et al. 2008). For example, comparison of X-ray (Gamble et al. 1997; Worthylake et al. 1999) and NMR (Byeon et al. 2009) structures of full-affinity CA^{CTD} dimers reveals slight variations in the structure of the dimerization helix, which occur at both the tertiary level (in terms of helix 9 packing against other helices in the same domain) and quaternary level (in terms of the helix 9 crossing angle across the dimer dyad) (Fig. 11c). Flexibility of the CA^{CTD} dimer might

have functional implications since twisting at the dimer interface may also dictate lattice curvature (indicated by red double-headed arrows in Fig. 11c) (Ternois et al. 2005; Ganser-Pornillos et al. 2007). Indeed, computational modeling of the HIV-1 capsid suggests that proper formation of the pentameric declinations requires a flexible dimer interface (Pornillos et al. 2011).

An electron cryomicroscopy reconstruction of helical tubes composed of HIV-1 CA hexamers indicates that adjacent CA^{CTD} domains surrounding the threefold axes of the hexagonal lattice may also interact via extended polar residues (Byeon et al. 2009). This interaction is not observed in structures of flattened lattices of CA (Ganser-Pornillos et al. 2007) and, therefore, appears to specifically stabilize subunit packing in a curved lattice. In the assembled capsid, it is likely that interactions across the threefold interface vary in response to different degrees of rotation at the NTD–CTD interface (Byeon et al. 2009; Pornillos et al. 2009).

6. Organization of the RNA Genome

The morphological and structural rearrangements that occur during retroviral maturation likely prepare the RNA genome for proper replication upon cell entry. Consistent with this idea, the genome itself undergoes structural rearrangements during maturation, in which the RNA condenses with the new NC proteins inside the capsid and adopts a more stable structure (Fu and Rein 1993). Furthermore, there appears to be a structural link between the genome and the capsid shell because alterations in capsid stability can significantly perturb reverse transcription (Forshey et al. 2002). Very little is currently known about the three-dimensional organization of the genome within the core, but significant progress has been made in delineating the secondary structural elements (Watts et al. 2009). This is an exciting unexplored area in retrovirus structure.

7. Conserved and Contrasting Features in the Design of Enveloped Spherical Viruses

As molecular machines, viruses have evolved efficient, elegant methods to perform their vital functions: (1) protect the genome upon exit from an infected cell, (2) recognize a susceptible host cell and trigger an entry mechanism, and (3) co-opt normal cellular machinery to replicate and assemble progeny. For retroviruses, and in fact most viruses, the first function is accomplished by the capsid, a protective protein shell with tightly packed subunits that exclude harmful proteins such as ribonucleases, and the second function is accomplished by trimeric Env glycoprotein spikes which recognize specific cellular receptors and mediate fusion of the viral envelope with the cell membrane.

The structures of the capsids and surface proteins from many enveloped viruses are now known and have begun to reveal both common and diverging features in virus architecture. As might be expected, many enveloped viruses have capsids and/or envelope proteins organized by the classical principles of icosahedral symmetry. The most striking example of this is the alphavirus family, where even the lipid bilayer of the virion is constrained to icosahedral symmetry (Zhang et al. 2002). On the other hand, hepatitis B virus does have an

icosahedral capsid but also a pleomorphic envelope with a relatively random distribution of spikes (Dryden et al. 2006). Nevertheless, the envelope and capsid reside in close proximity, and the surface L protein mediates intimate interactions with the internal capsid. Like hepatitis B virus, herpesvirus has a pleomorphic envelope and an icosahedral inner capsid. However, a disordered tegument protein shell resides between the envelope and capsid (Grünewald et al. 2003). Finally, orthoretroviruses appear to be an extreme case of pleomorphism because both the capsids and surface glycoproteins are nonicosahedral.

This pleomorphism has made structural analyses of orthoretroviral capsids and envelope proteins very difficult. This chapter illustrates the “bottoms-up” approach that has been used to study these types of structures, wherein high-resolution information on the building blocks are coupled with lower-resolution electron microscopy structures and functional data to build models for the complete capsid. This approach requires close collaborations between structural biologists, biochemists, and virologists.

8. Future Directions

Future directions for studies of orthoretroviral capsid assembly include determination of higherresolution structures of the immature Gag lattice, characterization of the molecular rearrangements (both within the RNA genome and the capsid shells) that occur during the regulated maturation of the virus, and dissection of the early events in the viral replication cycle. Of particular interest are the fate of the viral capsid once it enters the cell and how the capsid and its contents reorganize to form the enzymatic complex that reverse transcribes the genome and targets it to host chromosomes for integration.

Acknowledgments

HIV research in the Yeager laboratory is supported by grants from the US National Institutes of Health (R01-GM066087 and P50-GM082545). We thank John Briggs, Rebecca Craven, Alasdair Steven, and Elizabeth Wright for generously supplying materials for figures; Kelly Dryden and Jeong-Hyun Lee for assistance in preparing figures; and Wes Sundquist for helpful discussions. We apologize to colleagues whose works were not cited due to lack of space or inadvertent omission.

References

Accola MA, Höglund S, Göttlinger HG (1998) A putative a-helical structure which overlaps the capsid-p2 boundary in the human immunodeficiency virus type 1 Gag precursor is crucial for viral particle assembly. J Virol 72:2072–2078 [PubMed: 9499062]

Alcaraz LA, del Álamo M, Barrera FN et al. (2007) Flexibility in HIV-1 assembly subunits: solution structure of the monomeric C-terminal domain of the capsid protein. Biophys J 93:1264–1276 [PubMed: 17526561]

Aloia RC, Tian H, Jensen FC (1993) Lipid composition and fluidity of the human immunodeficiency virus envelope and host cell plasma membranes. Proc Natl Acad Sci USA 90:5181–5185 [PubMed: 8389472]

Bailey GD, Hyun JK, Mitra AK et al. (2009) Proton-linked dimerization of a retroviral capsid protein initiates capsid assembly. Structure 17:737–748 [PubMed: 19446529]

Bajorek M, Schubert HL, McCullough J et al. (2009) Structural basis for ESCRT-III protein autoinhibition. Nat Struct Mol Biol 16:754–762 [PubMed: 19525971]

Bartonova V, Igonet S, Sticht J et al. (2008) Residues in the HIV-1 capsid assembly inhibitor binding site are essential for maintaining the assembly-competent quaternary structure of the capsid protein. J Biol Chem 283:32024–32033 [PubMed: 18772135]

Benjamin J, Ganser-Pornillos BK, Tivol WF et al. (2005) Three-dimensional structure of HIV-1 virus-like particles by electron cryotomography. J Mol Biol 346:577–588 [PubMed: 15670606]

Bouamr F, Melillo JA, Wang MQ et al. (2003) PPPYEPTAP motif is the late domain of human T-cell leukemia virus type 1 Gag and mediates its functional interaction with cellular proteins Nedd4 and Tsg101. J Virol 77:11882–11895 [PubMed: 14581525]

Bowzard JB, Wills JW, Craven RC (2001) Second-site suppressors of Rous sarcoma virus CA mutations: evidence for interdomain interactions. J Virol 75:6850–6856 [PubMed: 11435564]

Briggs JAG, Wilk T, Welker R et al. (2003) Structural organization of authentic, mature HIV-1 virions and cores. EMBO J 22:1707–1715 [PubMed: 12660176]

Briggs JA, Grünewald K, Glass B et al. (2006) The mechanism of HIV-1 core assembly: insights from three-dimensional reconstructions of authentic virions. Structure 14:15–20 [PubMed: 16407061]

Briggs JAG, Riches JD, Glass B et al. (2009) Structure and assembly of immature HIV. Proc Natl Acad Sci USA 106:11090–11095 [PubMed: 19549863]

Brown DA, London E (1997) Structure of detergent-resistant membrane domains: does phase separation occur in biological membranes? Biochem Biophys Res Commun 240:1–7 [PubMed: 9367871]

Brügger B, Glass B, Haberkant P et al. (2006) The HIV lipidome: a raft with an unusual composition. Proc Natl Acad Sci USA 103:2641–2646 [PubMed: 16481622]

Butan C, Winkler DC, Heymann JB et al. (2008) RSV capsid polymorphism correlates with polymerization efficiency and envelope glycoprotein content: implications that nucleation controls morphogenesis. J Mol Biol 376:1168–1181 [PubMed: 18206161]

Byeon I-JL, Meng X, Jung J et al. (2009) Structural convergence between cryo-EM and NMR reveals intersubunit interactions critical for HIV-1 capsid function. Cell 139:780–790 [PubMed: 19914170]

Campbell S, Rein A (1999) In vitro assembly properties of human immunodeficiency virus type 1 Gag protein lacking the p6 domain. J Virol 73:2270–2279 [PubMed: 9971810]

Campbell S, Vogt VM (1995) Self-assembly in vitro of purified CA-NC proteins from Rous sarcoma virus and human immunodeficiency virus type 1. J Virol 69:6487–6497 [PubMed: 7666550]

Campbell S, Vogt VM (1997) In vitro assembly of virus-like particles with Rous sarcoma virus Gag deletion mutants: identification of the p10 domain as a morphological determinant in the formation of spherical particles. J Virol 71:4425–4435 [PubMed: 9151833]

Campbell S, Fisher RJ, Towler EM et al. (2001) Modulation of HIV-like particle assembly in vitro by inositol phosphates. Proc Natl Acad Sci USA 98:10875–10879 [PubMed: 11526217]

Campos-Olivas R, Newman JL, Summers MF (2000) Solution structure and dynamics of the Rous sarcoma virus capsid protein and comparison with capsid proteins of other retroviruses. J Mol Biol 296:633–649 [PubMed: 10669613]

Cardone G, Purdy JG, Cheng N et al. (2009) Visualization of a missing link in retrovirus capsid assembly. Nature 457:694–698 [PubMed: 19194444]

Carlson L-A, Briggs JAG, Glass B et al. (2008) Three-dimensional analysis of budding sites and released virus suggests a revised model for HIV-1 morphogenesis. Cell Host Microbe 4:592–599 [PubMed: 19064259]

Carlton JG, Martin-Serrano J (2007) Parallels between cytokinesis and retroviral budding: a role for the ESCRT machinery. Science 316:1908–1912 [PubMed: 17556548]

Caspar DLD, Klug A (1962) Physical principles in the construction of regular viruses. Cold Spring Harb Symp Quant Biol 27:1–24 [PubMed: 14019094]

Cheslock SR, Poon DTK, Fu W et al. (2003) Charged assembly helix motif in murine leukemia virus capsid: an important region for virus assembly and particle size determination. J Virol 77:7058–7066 [PubMed: 12768025]

Chung H-Y, Morita E, von Schwedler U et al. (2008) NEDD4L overexpression rescues the release and infectivity of human immunodeficiency virus type 1 constructs lacking PTAP and YPXL late domains. J Virol 82: 4884–4897 [PubMed: 18321968]

Dalton AK, Murray PS, Murray D et al. (2005) Biochemical characterization of Rous sarcoma virus MA protein interaction with membranes. J Virol 79:6227–6238 [PubMed: 15858007]

Dalton AK, Ako-Adjei D, Murray PS et al. (2007) Electrostatic interactions drive membrane association of the human immunodeficiency virus type 1 Gag MA domain. J Virol 81:6434–6445 [PubMed: 17392361]

Datta SAK, Curtis JE, Ratcliff W et al. (2007a) Conformation of the HIV-1 Gag protein in solution. J Mol Biol 365:812–824 [PubMed: 17097677]

Datta SAK, Zhao Z, Clark PK et al. (2007b) Interactions between HIV-1 Gag molecules in solution: an inositol phosphate-mediated switch. J Mol Biol 365:799–811 [PubMed: 17098251]

de Marco A, Davey NE, Ulbrich P et al. (2010) Conserved and variable features of Gag structure and arrangement in immature retrovirus particles. J Virol 84:11729–11736 [PubMed: 20810738]

Dey A, York D, Smalls-Mantey A et al. (2005) Composition and sequence-dependent binding of RNA to the nucleocapsid protein of Moloney murine leukemia virus. Biochemistry 44:3735–3744 [PubMed: 15751950]

Dorfman T, Mammano F, Haseltine WA et al. (1994) Role of the matrix protein in the virion association of the human immunodeficiency virus type 1 envelope glycoprotein. J Virol 68:1689–1696 [PubMed: 8107229]

Dryden KA, Wieland SF, Whitten-Bauer C et al. (2006) Native Hepatitis B virions and capsids visualized by electron cryomicroscopy. Mol Cell 22:843–850 [PubMed: 16793552]

D'Souza V, Summers MF (2004) Structural basis for packaging the dimeric genome of Moloney murine leukaemia virus. Nature 431:586–590 [PubMed: 15457265]

D'Souza V, Melamed J, Habib D et al. (2001) Identification of a high affinity nucleocapsid protein binding element within the Moloney murine leukemia virus Y-RNA packaging signal: implications for genome recognition. J Mol Biol 314:217–232 [PubMed: 11718556]

Ehrlich LS, Agresta BE, Carter CA (1992) Assembly of recombinant human immunodeficiency virus type 1 capsid protein in vitro. J Virol 66:4874–4883 [PubMed: 1629958]

Fabrikant G, Lata S, Riches JD et al. (2009) Computational model of membrane fission catalyzed by ESCRT-III. PLoS Comput Biol 5:e1000575

Forshey BM, von Schwedler U, Sundquist WI et al. (2002) Formation of a human immunodeficiency virus type 1 core of optimal stability is crucial for viral replication. J Virol 76:5667–5677 [PubMed: 11991995]

Freed EO, Martin MA (1995) Virion incorporation of envelope glycoproteins with long but not short cytoplasmic tails is blocked by specific, single amino acid substitutions in the human immunodeficiency virus type 1 matrix. J Virol 69:1984–1989 [PubMed: 7853546]

Freed EO, Martin MA (1996) Domains of the human immunodeficiency virus type 1 matrix and gp41 cytoplasmic tail required for envelope incorporation into virions. J Virol 70:341–351 [PubMed: 8523546]

Fu W, Rein A (1993) Maturation of dimeric viral RNA of Moloney murine leukemia virus. J Virol 67:5443–5449 [PubMed: 8350405]

Fuller SD, Wilk T, Gowen BE et al. (1997) Cryo-electron microscopy reveals ordered domains in the immature HIV-1 particle. Curr Biol 7:729–738 [PubMed: 9368755]

Gamble TR, Yoo S, Vajdos FF et al. (1997) Structure of the carboxyl-terminal dimerization domain of the HIV-1 capsid protein. Science 278:849–853 [PubMed: 9346481]

Ganser BK, Li S, Klishko VY et al. (1999) Assembly and analysis of conical models for the HIV-1 core. Science 283:80–83 [PubMed: 9872746]

Ganser-Pornillos BK, von Schwedler UK, Stray KM et al. (2004) Assembly properties of the human immunodeficiency virus type 1 CA protein. J Virol 78:2545–2552 [PubMed: 14963157]

Ganser-Pornillos BK, Cheng A, Yeager M (2007) Structure of full-length HIV-1 CA: a model for the mature capsid lattice. Cell 131:70–79 [PubMed: 17923088]

Ganser-Pornillos BK, Yeager M, Sundquist WI (2008) The structural biology of HIV assembly. Curr Opin Struct Biol 18:203–217 [PubMed: 18406133]

Garrus JE, von Schwedler UK, Pornillos O et al. (2001) Tsg101 and the vacuolar protein sorting pathway are essential for HIV-1 budding. Cell 107:55–65 [PubMed: 11595185]

Ghazi-Tabatabai S, Saksena S, Short JM et al. (2008) Structure and disassembly of filaments formed by the ESCRT-III subunit Vps24. Structure 16:1345–1356 [PubMed: 18786397]

Gherghe C, Lombo T, Leonard CW et al. (2010) Definition of a high-affinity Gag recognition structure mediating packaging of a retroviral RNA genome. Proc Natl Acad Sci USA 107:19248–19253 [PubMed: 20974908]

Gheysen D, Jacobs E, de Foresta F et al. (1989) Assembly and release of HIV-1 precursor $Pr55^{gag}$ virus-like particles from recombinant baculovirus-infected insect cells. Cell 59:103–112 [PubMed: 2676191]

Gitti RK, Lee BM, Walker J et al. (1996) Structure of the amino-terminal core domain of the HIV-1 capsid protein. Science 273:231–235 [PubMed: 8662505]

Gottlinger HG, Sodroski JG, Haseltine WA (1989) Role of capsid precursor processing and myristoylation in morphogenesis and infectivity of human immunodeficiency virus type 1. Proc Natl Acad Sci USA 86:5781–5785 [PubMed: 2788277]

Gottlinger HG, Dorfman T, Sodroski JG et al. (1991) Effect of mutations affecting the p6 gag protein on human immunodeficiency virus particle release. Proc Natl Acad Sci USA 88:3195–3199 [PubMed: 2014240]

Gross I, Hohenberg H, Kräusslich H-G (1997) In vitro assembly properties of purified bacterially expressed capsid proteins of human immunodeficiency virus. Eur J Biochem 249:592–600 [PubMed: 9370371]

Gross I, Hohenberg H, Huckhagel C et al. (1998) N-terminal extension of human immunodeficiency virus capsid protein converts the in vitro assembly phenotype from tubular to spherical particles. J Virol 72:4798–4810 [PubMed: 9573245]

Gross I, Hohenberg H, Wilk T et al. (2000) A conformational switch controlling HIV-1 morphogenesis. EMBO J 19:103–113 [PubMed: 10619849]

Grünewald K, Desai P, Winkler DC et al. (2003) Three-dimensional structure of herpes simplex virus from cryo-electron tomography. Science 302:1396–1398 [PubMed: 14631040]

Hanson PI, Roth R, Lin Y et al. (2008) Plasma membrane deformation by circular arrays of ESCRT-III protein filaments. J Cell Biol 180:389–402 [PubMed: 18209100]

Hermida-Matsumoto L, Resh MD (2000) Localization of human immunodeficiency virus type 1 Gag and Env at the plasma membrane by confocal imaging. J Virol 74:8670–8679 [PubMed: 10954568]

Heymann JB, Butan C, Winkler DC et al. (2008) Irregular and semi-regular polyhedral models for Rous sarcoma virus cores. Comput Math Methods Med 9:197–210 [PubMed: 19122884]

Hill CP, Worthylake D, Bancroft DP et al. (1996) Crystal structures of the trimeric human immunodeficiency virus type 1 matrix protein: implications for membrane association and assembly. Proc Natl Acad Sci USA 93:3099–3104 [PubMed: 8610175]

Hurley JH, Emr SD (2006) The ESCRT complexes: structure and mechanism of a membrane-trafficking network. Annu Rev Biophys Biomol Struct 35:277–298 [PubMed: 16689637]

Hyun J- K, Radjainia M, Kingston RL et al. (2010) Proton-driven assembly of the Rous sarcoma virus capsid protein results in the formation of icosahedral particles. J Biol Chem 285:15056–15064 [PubMed: 20228062]

Ivanchenko S, Godinez WJ, Lampe M et al. (2009) Dynamics of HIV-1 assembly and release. PLoS Pathog 5:e1000652

Ivanov D, Tsodikov OV, Kasanov J et al. (2007) Domain-swapped dimerization of the HIV-1 capsid C-terminal domain. Proc Natl Acad Sci USA 104:4353–4358 [PubMed: 17360528]

Jin Z, Jin L, Peterson DL et al. (1999) Model for lentivirus capsid core assembly based on crystal dimers of EIAV p26. J Mol Biol 286:83–93 [PubMed: 9931251]

Joint United Nations Programme on HIV/AIDS (2009) AIDS epidemic update. UNAIDS, Geneva

Joshi SM, Vogt VM (2000) Role of the Rous sarcoma virus p10 domain in shape determination of Gag virus-like particles assembled in vitro and within Escherichia coli. J Virol 74:10260–10268 [PubMed: 11024160]

Jouvenet N, Bieniasz PD, Simon SM (2008) Imaging the biogenesis of individual HIV-1 virions in live cells. Nature 454:236–240 [PubMed: 18500329]

Jouvenet N, Simon SM, Bieniasz PD (2009) Imaging the interaction of HIV-1 genomes and Gag during assembly of individual viral particles. Proc Natl Acad Sci USA 106:19114–19119 [PubMed: 19861549]

Keller PW, Johnson MC, Vogt VM (2008) Mutations in the spacer peptide and adjoining sequences in Rous sarcoma virus Gag lead to tubular budding. J Virol 82:6788–6797 [PubMed: 18448521]

Keller PW, Adamson CS, Heymann JB et al. (2011) HIV-1 maturation inhibitor bevirimat stabilizes the immature Gag lattice. J Virol 85:1420–1428 [PubMed: 21106735]

Kelly BN, Howard BR, Wang H et al. (2006) Implications for viral capsid assembly from crystal structures of HIV-1 Gag and CA^N. Biochemistry 45:11257–11266 1–278 133–278 [PubMed: 16981686]

Khorasanizadeh S, Campos-Olivas R, Summers MF (1999) Solution structure of the capsid protein from the human T-cell leukemia virus type-I. J Mol Biol 291:491–505 [PubMed: 10438634]

Kikonyogo A, Bouamr F, Vana ML et al. (2001) Proteins related to the Nedd4 family of ubiquitin protein ligases interact with the L domain of Rous sarcoma virus and are required for gag budding from cells. Proc Natl Acad Sci USA 98:11199–11204 [PubMed: 11562473]

Kingston RL, Fitzon-Ostendorp T, Eisenmesser EZ et al. (2000) Structure and self-association of the Rous sarcoma virus capsid protein. Structure 8:617–628 [PubMed: 10873863]

Knejzlík Z, Smékalová Z, Ruml T et al. (2007) Multimerization of the p12 domain is necessary for Mason-Pfizer monkey virus Gag assembly in vitro. Virology 365:260–270 [PubMed: 17490704]

Kräusslich H-G (1991) Human immunodeficiency virus proteinase dimer as component of the viral polyprotein pre-vents particle assembly and viral infectivity. Proc Natl Acad Sci USA 88:3213–3217 [PubMed: 2014242]

Kräusslich H-G, Fäcke M, Heuser A-M et al. (1995) The spacer peptide between human immunodeficiency virus capsid and nucleocapsid proteins is essential for ordered assembly and viral infectivity. J Virol 69:3407–3419 [PubMed: 7745687]

Lanman J, Lam TT, Barnes S et al. (2003) Identification of novel interactions in HIV-1 capsid protein assembly by high-resolution mass spectrometry. J Mol Biol 325:759–772 [PubMed: 12507478]

Lanman J, Lam TT, Emmett MR et al. (2004) Key interactions in HIV-1 maturation identified by hydrogen-deuterium exchange. Nat Struct Mol Biol 11:676–677 [PubMed: 15208693]

Lapatto R, Blundell T, Hemmings A et al. (1989) X-ray analysis of HIV-1 proteinase at 2.7 Å resolution confirms structural homology among retroviral enzymes. Nature 342:299–302 [PubMed: 2682266]

Lata S, Schoehn G, Jain A et al. (2008) Helical structures of ESCRT-III are disassembled by VPS4. Science 321:1354–1357 [PubMed: 18687924]

Le Blanc I, Prévost M-C, Dokhélar M-C et al. (2002) The PPPY motif of human T-cell leukemia virus type 1 Gag protein is required early in the budding process. J Virol 76:10024–10029 [PubMed: 12208980]

Li S, Hill CP, Sundquist WI et al. (2000) Image reconstructions of helical assemblies of the HIV-1 CA protein. Nature 407:409–413 [PubMed: 11014200]

Li F, Goila-Gaur R, Salzwedel K et al. (2003) PA-457: a potent HIV inhibitor that disrupts core condensation by targeting a late step in Gag processing. Proc Natl Acad Sci USA 100:13555–13560 [PubMed: 14573704]

Li H, Dou J, Ding L et al. (2007) Myristoylation is required for human immunodeficiency virus type 1 Gag-Gag multimerization in mammalian cells. J Virol 81:12899–12910 [PubMed: 17881447]

Liang C, Hu J, Russell RS et al. (2002) Characterization of a putative a-helix across the capsid-SP1 boundary that is critical for the multimerization of human immunodeficiency virus type 1 Gag. J Virol 76:11729–11737 [PubMed: 12388733]

Lopez-Vergès S, Camus G, Blot G et al. (2006) Tail-interacting protein TIP47 is a connector between Gag and Env and is required for Env incorporation into HIV-1 virions. Proc Natl Acad Sci USA 103:14947–14952 [PubMed: 17003132]

Martin-Serrano J, Zang T, Bieniasz PD (2001) HIV-1 and Ebola virus encode small peptide motifs that recruit Tsg101 to sites of particle assembly to facilitate egress. Nat Med 7:1313–1319 [PubMed: 11726971]

Massiah MA, Starich MR, Paschall C et al. (1994) Three-dimensional structure of the human immunodeficiency virus type 1 matrix protein. J Mol Biol 244:198–223 [PubMed: 7966331]

Miyazaki Y, Garcia EL, King SR et al. (2010) An RNA structural switch regulates diploid genome packaging by Moloney murine leukemia virus. J Mol Biol 396:141–152 [PubMed: 19931283]

Monroe EB, Kang S, Kyere SK et al. (2010) Hydrogen/deuterium exchange analysis of HIV-1 capsid assembly and maturation. Structure 18:1483–1491 [PubMed: 21070947]

Morellet N, Druillennec S, Lenoir C et al. (2005) Helical structure determined by NMR of the HIV-1 (345–392) Gag sequence, surrounding p2: implications for particle assembly and RNA packaging. Protein Sci 14:375–386 [PubMed: 15659370]

Morita E, Sandrin V, Chung H-Y et al. (2007) Human ESCRT and ALIX proteins interact with proteins of the midbody and function in cytokinesis. EMBO J 26:4215–4227 [PubMed: 17853893]

Mortuza GB, Haire LF, Stevens A et al. (2004) High-resolution structure of a retroviral capsid hexameric amino-terminal domain. Nature 431:481–485 [PubMed: 15386017]

Mortuza GB, Dodding MP, Goldstone DC et al. (2008) Structure of B-MLV capsid amino-terminal domain reveals key features of viral tropism, Gag assembly and core formation. J Mol Biol 376:1493–1508 [PubMed: 18222469]

Mortuza GB, Goldstone DC, Pashley C et al. (2009) Structure of the capsid amino-terminal domain from the betaretrovirus, Jaagsiekte sheep retrovirus. J Mol Biol 386:1179–1192 [PubMed: 19007792]

Müller B, Anders M, Akiyama H et al. (2009) HIV-1 Gag processing intermediates trans-dominantly interfere with HIV-1 infectivity. J Biol Chem 284:29692–29703 [PubMed: 19666477]

Murakami T, Freed EO (2000a) Genetic evidence for an interaction between human immunodeficiency virus type 1 matrix and a-helix 2 of the gp41 cytoplasmic tail. J Virol 74:3548–3554 [PubMed: 10729129]

Murakami T, Freed EO (2000b) The long cytoplasmic tail of gp41 is required in a cell type-dependent manner for HIV-1 envelope glycoprotein incorporation into virions. Proc Natl Acad Sci USA 97:343–348 [PubMed: 10618420]

Nandhagopal N, Simpson AA, Johnson MC et al. (2004) Dimeric Rous sarcoma virus capsid protein structure relevant to immature Gag assembly. J Mol Biol 335:275–282 [PubMed: 14659756]

Navia MA, Fitzgerald PMD, McKeever BM et al. (1989) Three-dimensional structure of aspartyl protease from human immunodeficiency virus HIV-1. Nature 337:6l5–620

Newman JL, Butcher EW, Patel DT et al. (2004) Flexibility in the P2 domain of the HIV-1 Gag polyprotein. Protein Sci 13:2101–2107 [PubMed: 15238640]

Nguyen DH, Hildreth JE (2000) Evidence for budding of human immunodeficiency virus type l selectively from glycolipid-enriched membrane lipid rafts. J Virol 74:3264–3272 [PubMed: 10708443]

Ono A, Freed EO (2001) Plasma membrane rafts play a critical role in HIV-1 assembly and release. Proc Natl Acad Sci USA 98:13925–13930 [PubMed: 11717449]

Ono A, Demirov D, Freed EO (2000) Relationship between human immunodeficiency virus type 1 Gag multimerization and membrane binding. J Virol 74:5142–5150 [PubMed: 10799589]

Ono A, Ablan SD, Lockett SJ et al. (2004) Phosphatidylinositol (4,5) bisphosphate regulates HIV-1 Gag targeting to the plasma membrane. Proc Natl Acad Sci USA 101:14889–14894 [PubMed: 15465916]

Paillart J-C, Göttlinger HG (1999) Opposing effects of human immunodeficiency virus type 1 matrix mutations support a myristyl switch model of Gag membrane targeting. J Virol 73:2604–2612 [PubMed: 10074105]

Pettit SC, Sheng N, Tritch R et al. (1998) The regulation of sequential processing of HIV-1 Gag by the viral protease. Adv Exp Med Biol 436:15–25 [PubMed: 9561194]

Phillips JM, Murray PS, Murray D et al. (2008) A molecular switch required for retrovirus assembly participates in the hexagonal immature lattice. EMBO J 27:1411–1420 [PubMed: 18401344]

Pornillos O, Alam SL, Davis DR et al. (2002) Structure of the TsglGl UEV domain in complex with the PTAP motif of the HIV-1 p6 protein. Nat Struct Biol 9:812–817 [PubMed: 12379843]

Pornillos O, Ganser-Pornillos BK, Kelly BN et al. (2009) X-ray structures of the hexameric building block of the HIV capsid. Cell l37:l282–l292

Pornillos O, Ganser-Pornillos BK, Banumathi S et al. (2010) Disulfide bond stabilization of the hexameric capsomer of human immunodeficiency virus. J Mol Biol 401:985–995 [PubMed: 20600115]

Pornillos O, Ganser-Pornillos BK, Yeager M (2011) Atomic-level modelling of the HIV capsid. Nature 469:424–427 [PubMed: 21248851]

Purdy JG, Flanagan JM, Ropson IJ et al. (2008) Critical role of conserved hydrophobic residues within the major homology region in mature retroviral capsid assembly. J Virol 82:595l–596l

Purdy JG, Flanagan JM, Ropson IJ et al. (2009) Retroviral capsid assembly: a role for the CA dimer in initiation. J Mol Biol 389:438–45l [PubMed: 19361521]

Reil H, Bukovsky AA, Gelderblom HR et al. (1998) Efficient HIV-1 replication can occur in the absence of the viral matrix protein. EMBO J 17:2699–2708 [PubMed: 9564051]

Rumlova-Klikova M, Hunter E, Nermut MV et al. (2000) Analysis of Mason-Pfizer monkey virus Gag domains required for capsid assembly in bacteria: role of the N-terminal proline residue of CA in directing particle shape. J Virol 74:8452–8459 [PubMed: 10954545]

Saad JS, Miller J, Tai J et al. (2006) Structural basis for targeting HIV-1 Gag proteins to the plasma membrane for virus assembly. Proc Natl Acad Sci USA 103:11364–11369 [PubMed: 16840558]

Spearman P, Wang J-J, Heyden NV et al. (1994) Identification of human immunodeficiency virus type 1 Gag protein domains essential to membrane binding and particle assembly. J Virol 68:3232–3242 [PubMed: 8151785]

Spearman P, Horton R, Ratner L et al. (1997) Membrane binding of human immunodeficiency virus type 1 matrix protein in vivo supports a conformational myristyl switch mechanism. J Virol 71:6582–6592 [PubMed: 9261380]

Strack B, Calistri A, Craig S et al. (2003) AIP1/ALIX is a binding partner for HIV-1 p6 and EIAV p9 functioning in virus budding. Cell 114:689–699 [PubMed: 14505569]

Swanstrom R, Wills JW (1997) Synthesis, assembly and processing of viral proteins In: Coffin JM, Hughes SH, Varmus HE (eds) Retroviruses. Cold Spring Harbor Laboratory Press, New York

Tang C, Ndassa Y, Summers MF (2002) Structure of the N-terminal 283-residue fragment of the immature HIV-1 Gag polyprotein. Nat Struct Biol 9:537–543 [PubMed: 12032547]

Tang C, Loeliger E, Luncsford P et al. (2004) Entropic switch regulates myristate exposure in the HIV-1 matrix protein. Proc Natl Acad Sci USA 101:517–522 [PubMed: 14699046]

Ternois F, Sticht J, Duquerroy S et al. (2005) The HIV-1 capsid protein C-terminal domain in complex with a virus assembly inhibitor. Nat Struct Mol Biol 12:678–682 [PubMed: 16041386]

Tritch RJ, Cheng Y-SE, Yin FH et al. (1991) Mutagenesis of protease cleavage sites in the human immunodeficiency virus type 1 Gag polyprotein. J Virol 65:922–930 [PubMed: 1987379]

Usami Y, Popov S, Popova E et al. (2008) Efficient and specific rescue of human immunodeficiency virus type 1 bud-ding defects by a Nedd4-like ubiquitin ligase. J Virol 82:4898–4907 [PubMed: 18321969]

VerPlank L, Bouamr F, LaGrassa TJ et al. (2001) Tsg101, a homologue of ubiquitin-conjugating (E2) enzymes, binds the L domain in HIV type 1 Pr55Gag. Proc Natl Acad Sci USA 98:7724–7729 [PubMed: 11427703]

Vogt VM (1997) Retroviral virions and genomes In: Coffin JM, Hughes SH, Varmus HE (eds) Retroviruses. Cold Spring Harbor Laboratory Press, New York

von Schwedler UK, Stemmler TL, Klishko VY et al. (1998) Proteolytic refolding of the HIV-1 capsid protein amino-terminus facilitates viral core assembly. EMBO J 17:1555–1568 [PubMed: 9501077]

von Schwedler UK, Stray KM, Garrus JE et al. (2003a) Functional surfaces of the human immunodeficiency virus type 1 capsid protein. J Virol 77:5439–5450 [PubMed: 12692245]

von Schwedler UK, Stuchell M, Müller B et al. (2003b) The protein network of HIV budding. Cell 114:701–713 [PubMed: 14505570]

Wang C-T, Zhang Y, McDermott J et al. (1993) Conditional infectivity of a human immunodeficiency virus matrix domain deletion mutant. J Virol 67:7067–7076 [PubMed: 7693966]

Wang MQ, Kim W, Gao G et al. (2003) Endophilins interact with Moloney murine leukemia virus Gag and modulate virion production. J Biol 3:4 [PubMed: 14659004]

Watts JM, Dang KK, Gorelick RJ et al. (2009) Architecture and secondary structure of an entire HIV-1 RNA genome. Nature 460:711–716 [PubMed: 19661910]

Wiegers K, Rutter G, Kottler H et al. (1998) Sequential steps in human immunodeficiency virus particle maturation revealed by alterations of individual Gag polyprotein cleavage sites. J Virol 72:2846–2854 [PubMed: 9525604]

Wollert T, Wunder C, Lippincott-Schwartz J et al. (2009) Membrane scission by the ESCRT-III complex. Nature 458:172–177 [PubMed: 19234443]

Wong HC, Shin R, Krishna NR (2008) Solution structure of a double mutant of the carboxy-terminal dimerization domain of the HIV-1 capsid protein. Biochemistry 47:2289–2297 [PubMed: 18220423]

Worthylake DK, Wang H, Yoo S et al. (1999) Structures of the HIV-1 capsid protein dimerization domain at 2.6 Å resolution. Acta Crystallogr D Biol Crystallogr 55:85–92 [PubMed: 10089398]

Wright ER, Schooler JB, Ding HJ et al. (2007) Electron cryotomography of immature HIV-1 virions reveals the structure of the CA and SP1 Gag shells. EMBO J 26:2218–2226 [PubMed: 17396149]

Yasuda J, Hunter E, Nakao M et al. (2002) Functional involvement of a novel Nedd4-like ubiquitin ligase on retrovirus budding. EMBO Rep 3:636–640 [PubMed: 12101095]

Yeager M, Wilson-Kubalek EM, Weiner SG et al. (1998) Supramolecular organization of immature and mature murine leukemia virus revealed by electron cryo-microscopy: implications for retroviral assembly mechanisms. Proc Natl Acad Sci USA 95:7299–7304 [PubMed: 9636143]

Yu X, Yuan X, Matsuda Z et al. (1992) The matrix protein of human immunodeficiency virus type 1 is required for incorporation of viral envelope protein into mature virions. J Virol 66:4966–4971 [PubMed: 1629961]

Zacharias DA, Violin JD, Newton AC et al. (2002) Partitioning of lipid-modified monomeric GFPs into membrane microdomains of live cells. Science 296:913–916 [PubMed: 11988576]

Zhai Q, Fisher RD, Chung H-Y et al. (2008) Structural and functional studies of ALIX interactions with YPX_nL late domains of HIV-1 and EIAV. Nat Struct Mol Biol 15:43–49 [PubMed: 18066081]

Zhang Y, Barklis E (1997) Effects of nucleocapsid mutations on human immunodeficiency virus assembly and RNA encapsidation. J Virol 71:6765–6776 [PubMed: 9261401]

Zhang W, Mukhopadhyay S, Pletnev SV et al. (2002) Placement of the structural proteins in Sindbis virus. J Virol 76:11645–11658 [PubMed: 12388725]

Zhou W, Parent LJ, Wills JW et al. (1994) Identification of a membrane-binding domain within the amino-terminal region of human immunodeficiency virus type 1 Gag protein which interacts with acidic phospholipids. J Virol 68:2556–2569 [PubMed: 8139035]

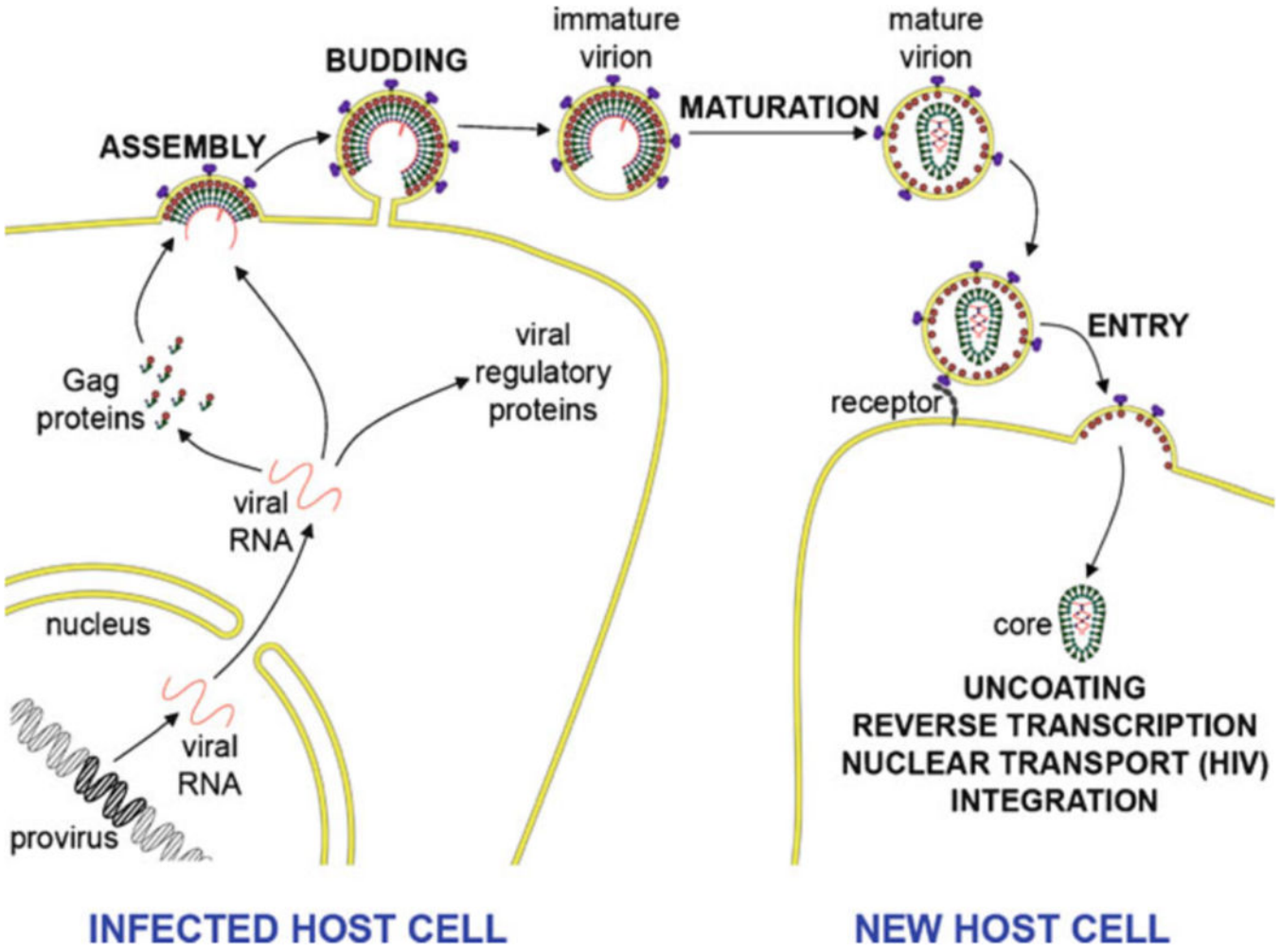

Fig. 1.

Schematic of the HIV-1 replication cycle, emphasizing the stages discussed in this chapter. See text for details. (Adapted from Ganser-Pornillos et al. (2008), with permission from Elsevier.)

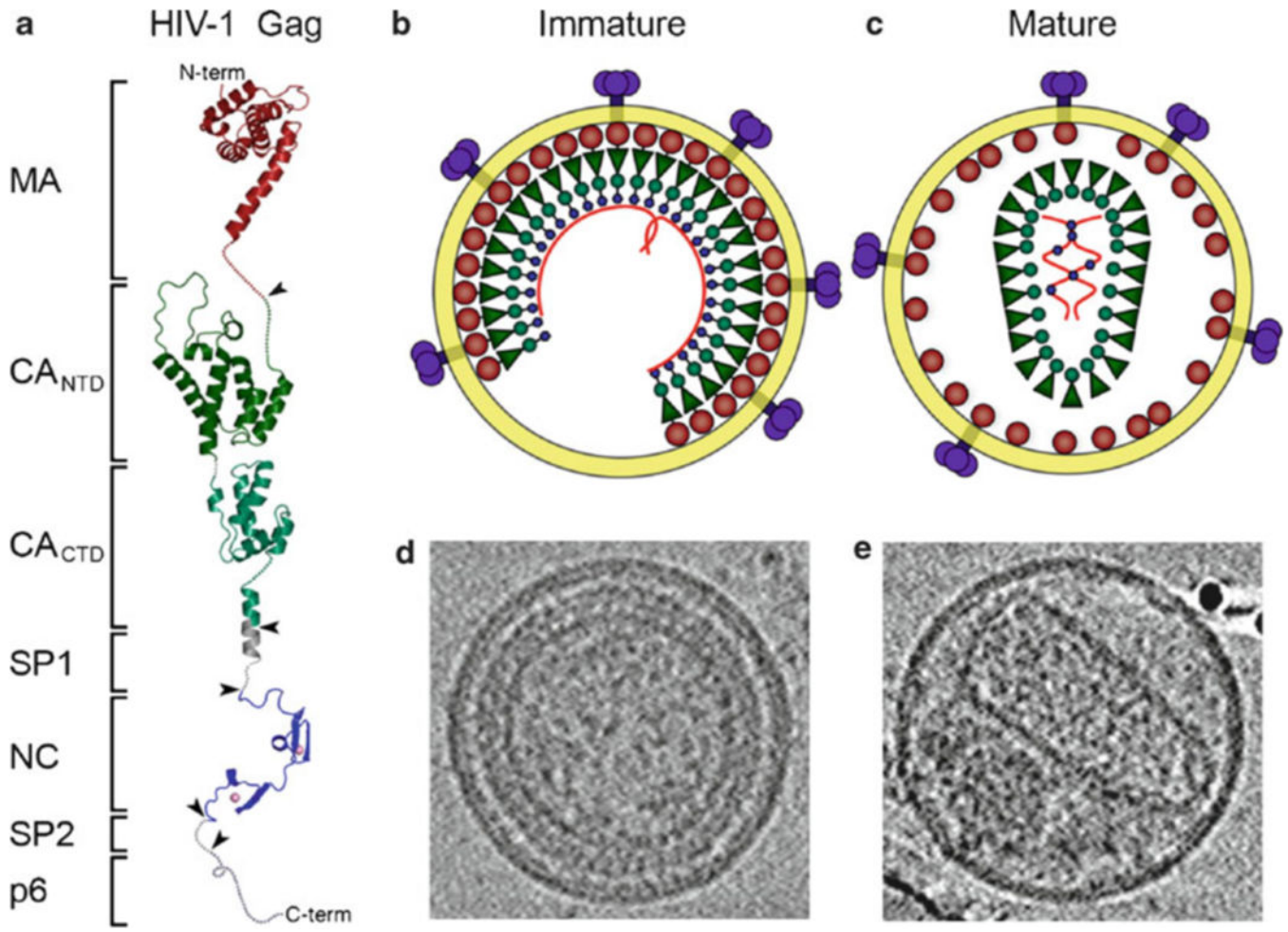

Fig. 2.

Organization of the immature and mature HIV-1 virions. (**a**) Schematic tertiary structural model of full-length HIV-1 Gag. Individual domains are in different colors and are labeled on the *left*. This color scheme is maintained throughout the chapter. (**b**) Schematic model of the immature virion. (**c**) Schematic model of the mature virion. Images of (**d**) immature and (**e**) mature virions preserved in vitreous ice. (Reprinted from Ganser-Pornillos et al. (2008), with permission from Elsevier.)

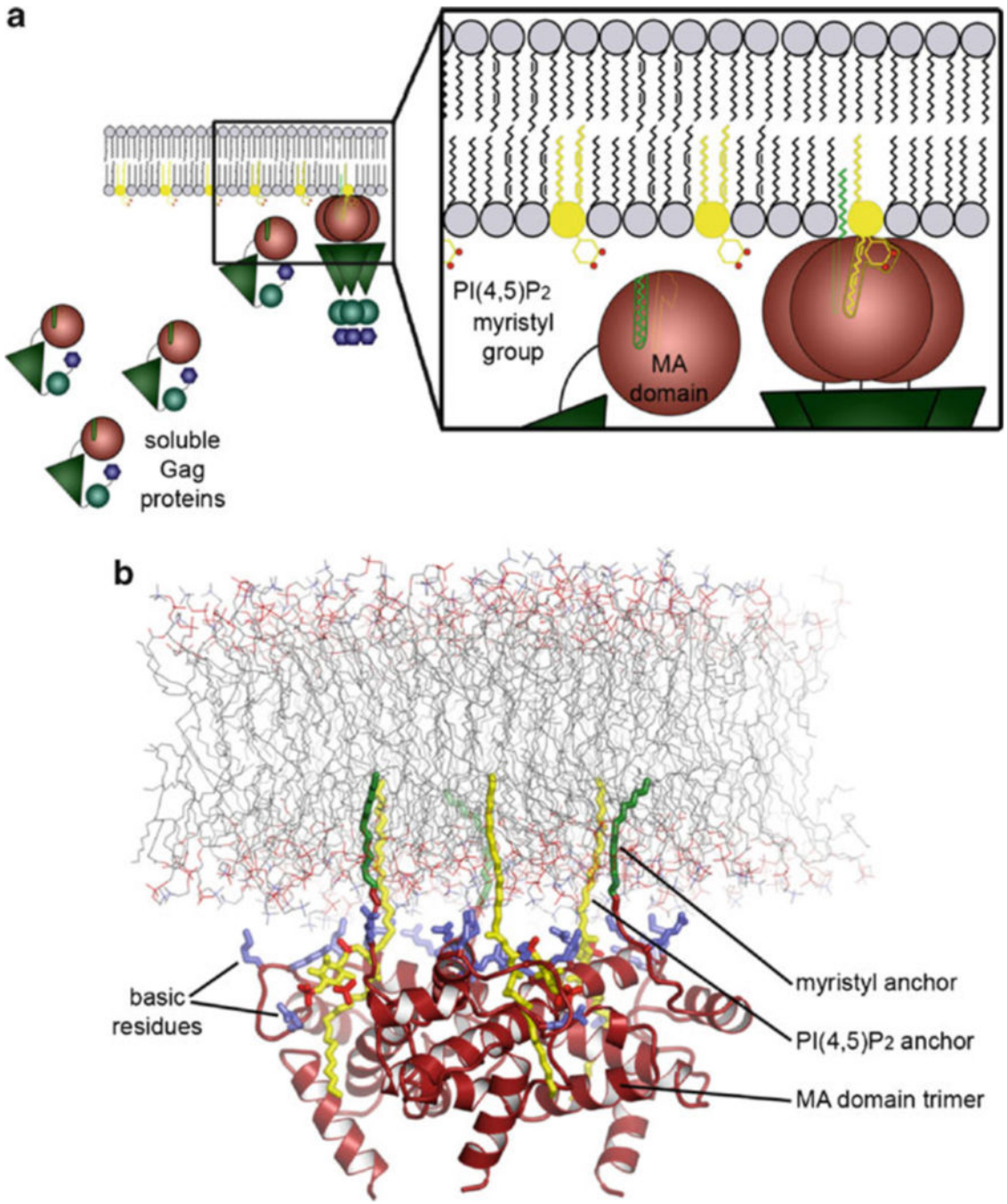

Fig. 3.

The MA domain functions in binding and targeting of Gag to the plasma membrane. (**a**) Schematic showing soluble Gag proteins in a "folded-over" conformation, and membrane-bound assembling Gag molecules in a "beads-on-a-string" configuration. The boxed region illustrates the "myristyl switch" mechanism of membrane binding. (**b**) Structural model of the MA trimer bound to the lipid bilayer. [(**b**) Reprinted from Ganser-Pornillos et al. (2008), with permission from Elsevier.]

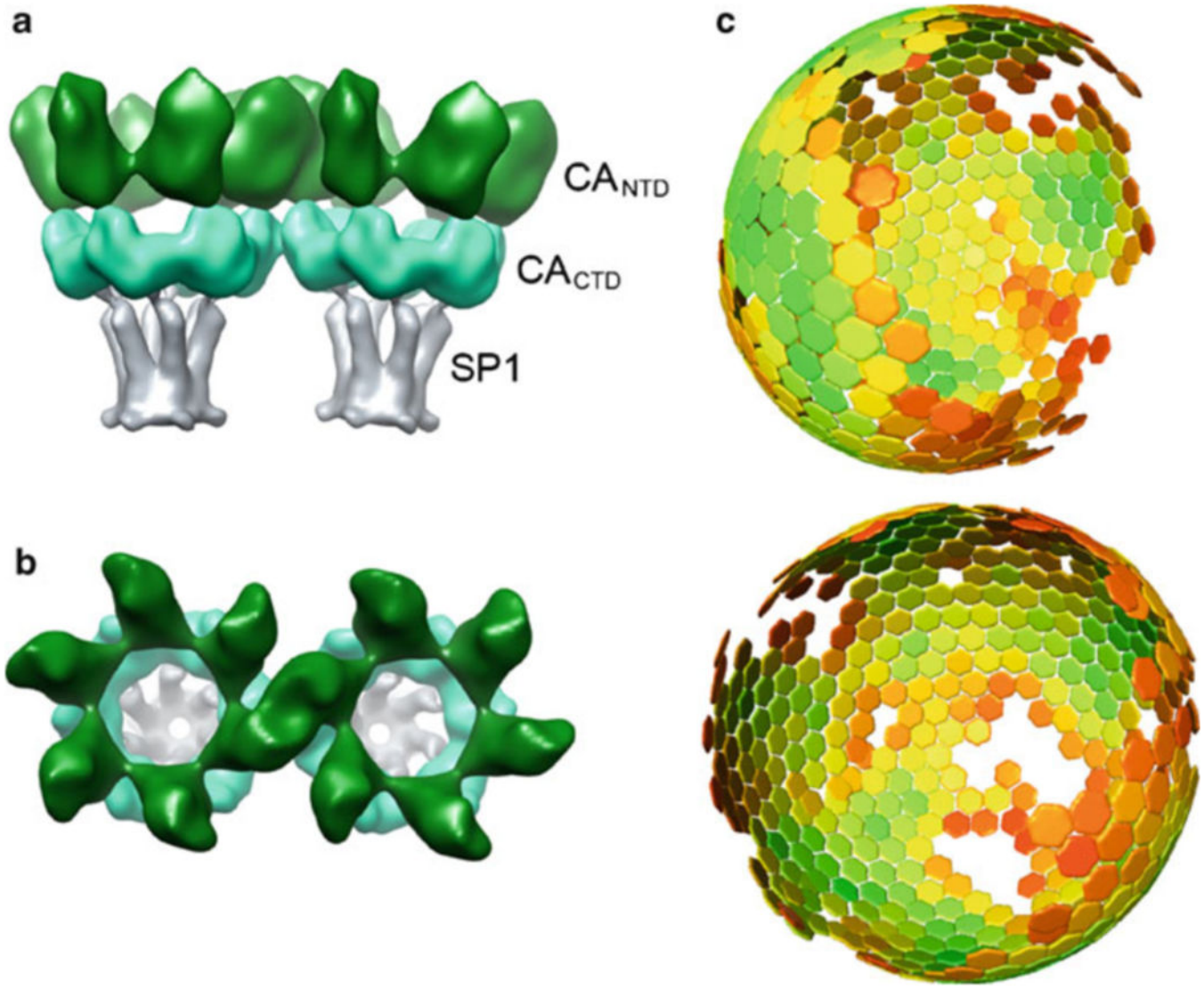

Fig. 4.

The immature Gag lattice. (**a**) Side view and (**b**) top view of a low-resolution model of two interacting Gag hexamers (Wright et al. 2007). The CA^{NTD}, CA^{CTD}, and SP1 layers are colored *green*, *cyan*, and *gray*, respectively. (Model used to generate images courtesy of Elizabeth Wright.) (**c**) Global map of the immature HIV-1 lattice (Briggs et al. 2009). The Gag hexamers are represented by hexagons and colored according to symmetry cross-correlation on a scale from low (*red*) to high (*green*). (Lattice map images courtesy of John Briggs.)

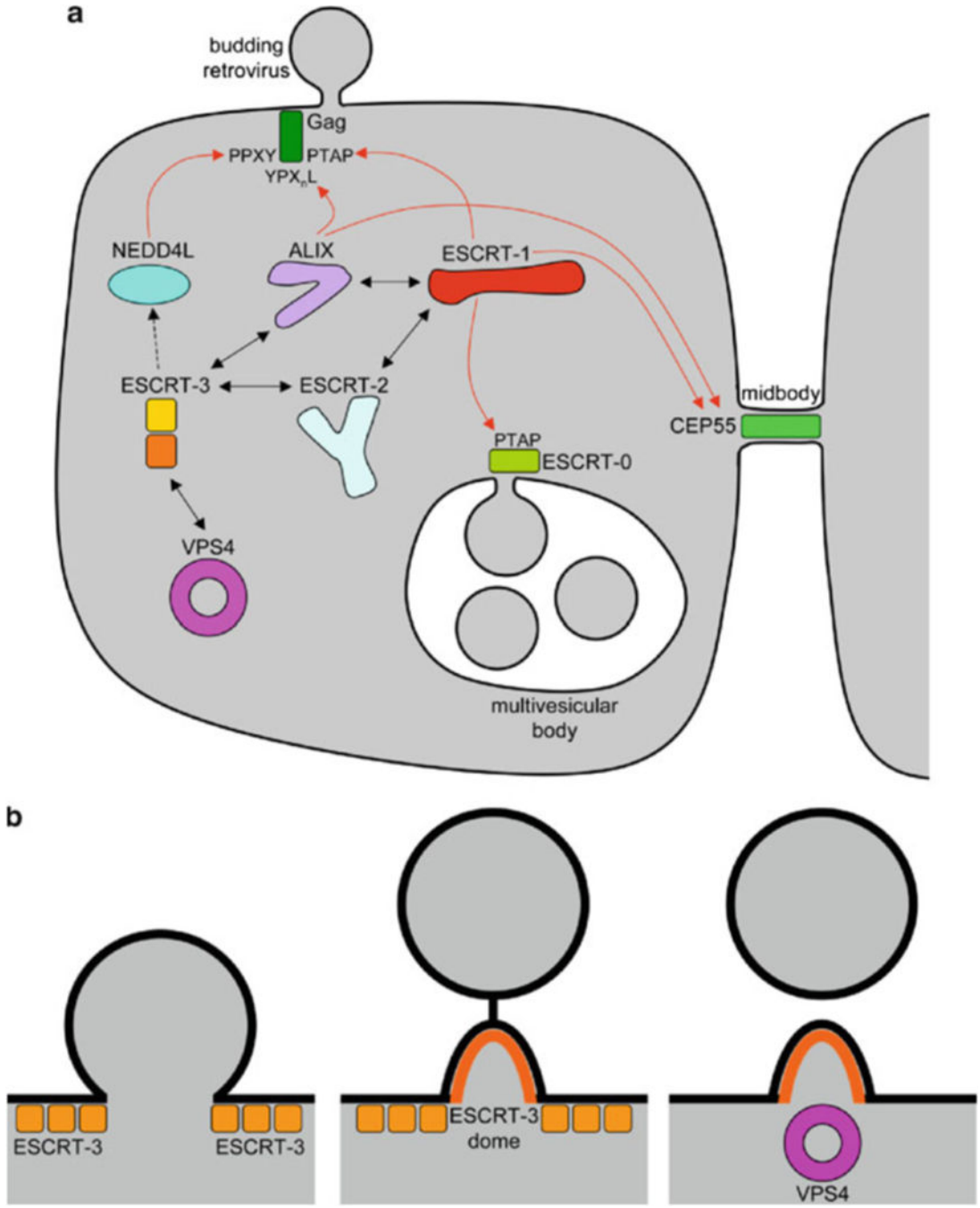

Fig. 5.

Retrovirus budding. (**a**) Schematic representation of the cellular ESCRT pathway. Known interactions between ESCRT complexes and ESCRT-associated proteins are indicated by the *black double-headed arrows*. *Red arrows* connect viral late domains or native cellular recruitment factors with their corresponding complex. Recruitment factors (viral Gag protein, ESCRT-0, and CEP55) are colored in *green shades*. Although it is known that recruitment of NEDD4L to viral budding sites leads to the eventual recruitment of ESCRT-III, the precise mechanism by which this occurs is not known. (**b**) Schematic representation

of the membrane fission mechanism catalyzed by ESCRT-III proteins and VPS4. (See text for details.)

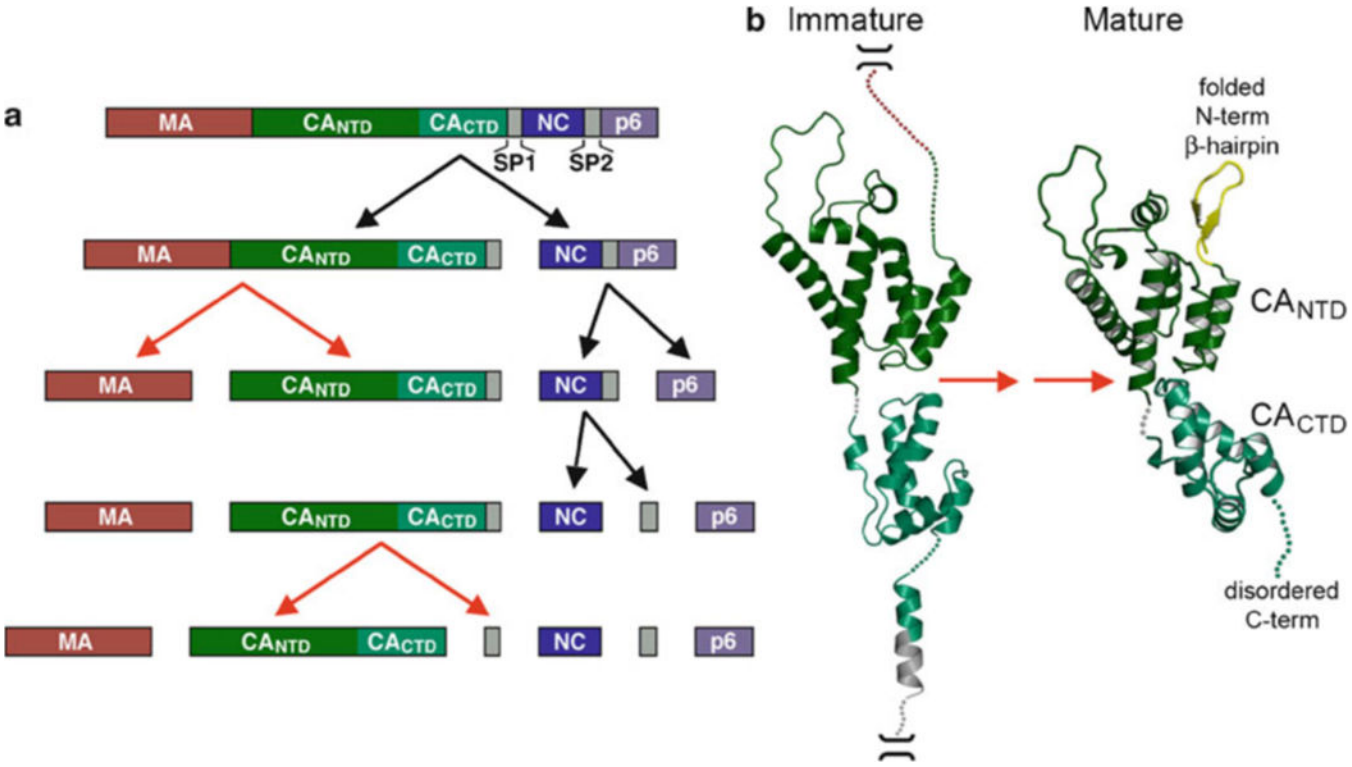

Fig. 6.

Proteolytic processing of Gag during maturation. (**a**) Schematic showing the HIV-1 Gag proteolysis cascade. Cleavage events that generate the mature CA termini are indicated by the *red arrows*. (**b**) Secondary and tertiary structural changes at the N-terminal and C-terminal ends of the CA domain. The depicted conformations of the MA/CA and CA/SP1 junctions in Gag are based on a variety of structural, biochemical, and mutagenesis studies. In mature CA, the Nterminal 13 residues are folded into a β-hairpin (colored *yellow*), and the C-terminal 11 residues are disordered. (Structure images reprinted from Ganser-Pornillos et al. (2008), with permission from Elsevier.)

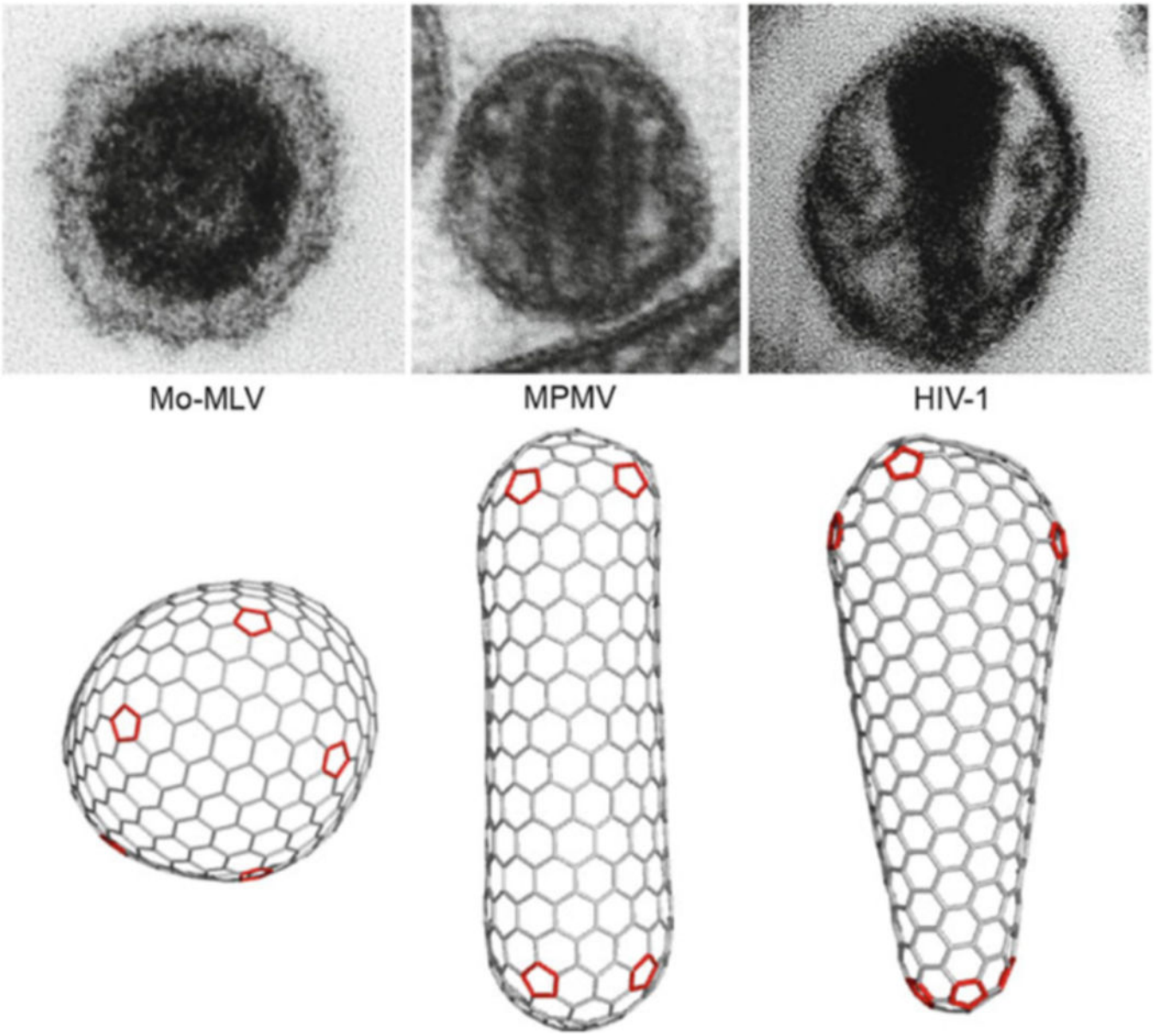

Fig. 7.

Morphologies of representative mature capsids of different orthoretroviruses. Images and fullerene models of Moloney murine leukemia virus (Mo-MLV, a gammaretrovirus), Mason-Pfizer monkey virus (MPMV, a betaretrovirus), and HIV-1 (a lentivirus) are shown. In all cases, the capsids are organized as fullerene structures that incorporate 12 pentamers (*red*) to close the hexagonal lattice. (Virus images reproduced from Ganser-Pornillos et al. (2004), with permission from American Society for Microbiology.)

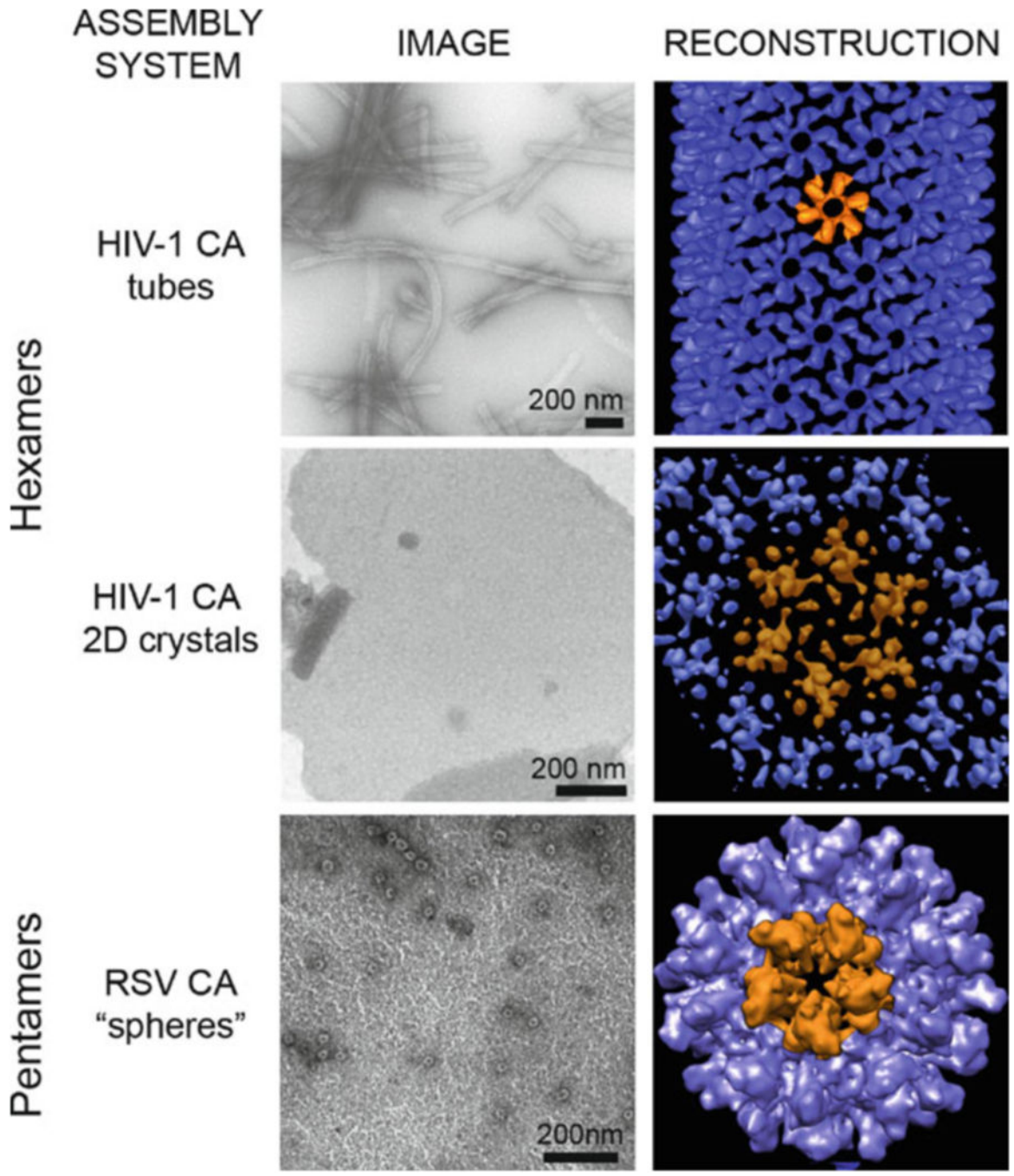

Fig. 8.

Gallery of *in vitro* assembly systems for retroviral capsids: helical tubes, two-dimensional hexagonal crystals, and icosahedral particles. (Images of HIV-1 assemblies reprinted from (Ganser-Pornillos et al. 2008), with permission from Elsevier. Image of RSV particles courtesy of Rebecca Craven. Reconstructed images of HIV-1 tubes reprinted from (Li et al. 2000), with permission from Macmillan Publishers Ltd. (Map used to generate T=1 image courtesy of Alasdair Steven.)

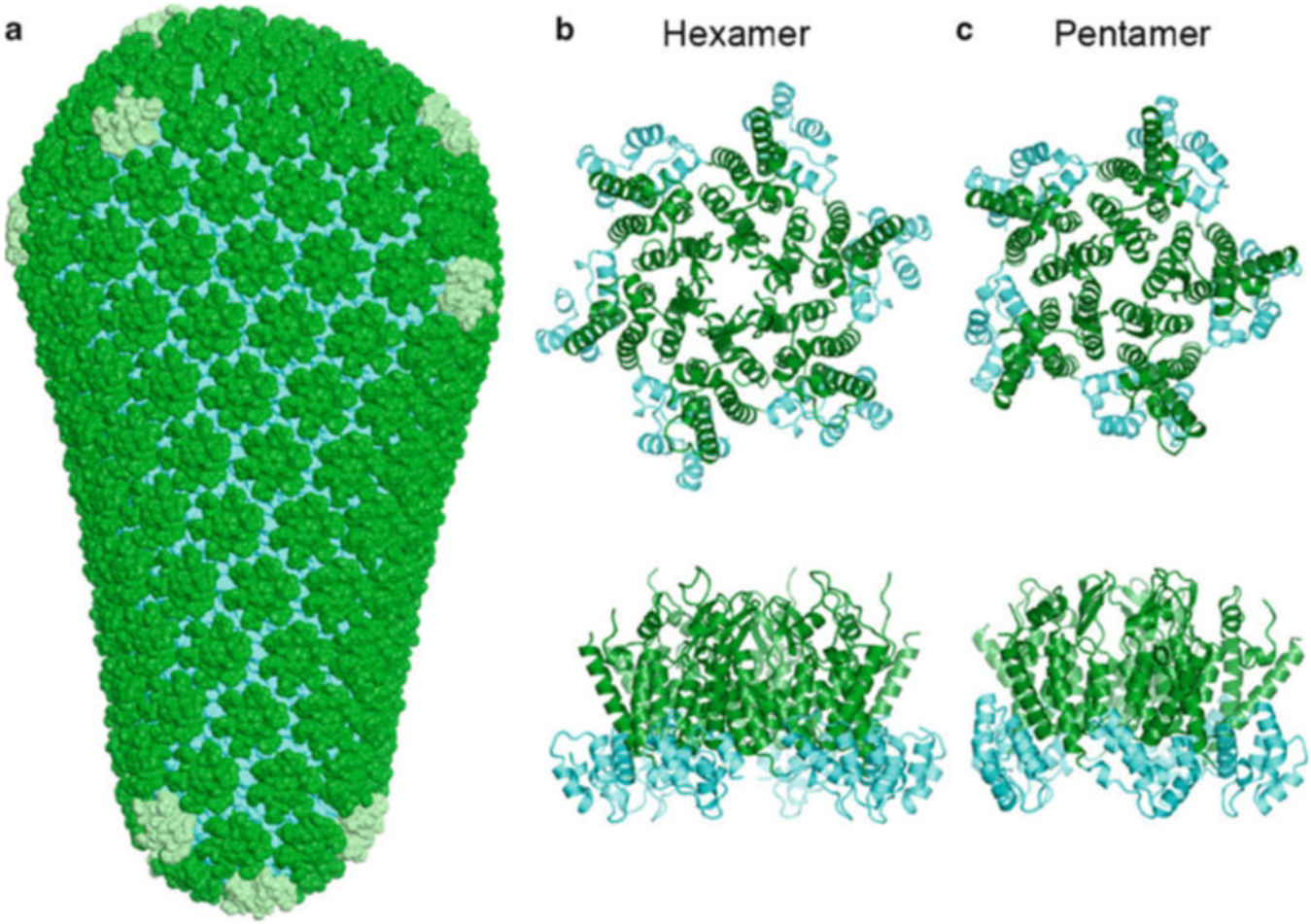

Fig. 9.

Organization of the mature HIV-1 capsid. (**a**) Structural model of the complete capsid, with the CA^{NTD} hexamers in *green*, CA^{NTD} pentamers in *light green*, and CA^{CTD} dimers in *cyan*. (**b**) Two views of the X-ray structure of the HIV-1 CA hexamer (Pornillos et al. 2009). (**c**) Two views of the X-ray structure of the HIV-1 CA pentamer (Pornillos et al. 2011).

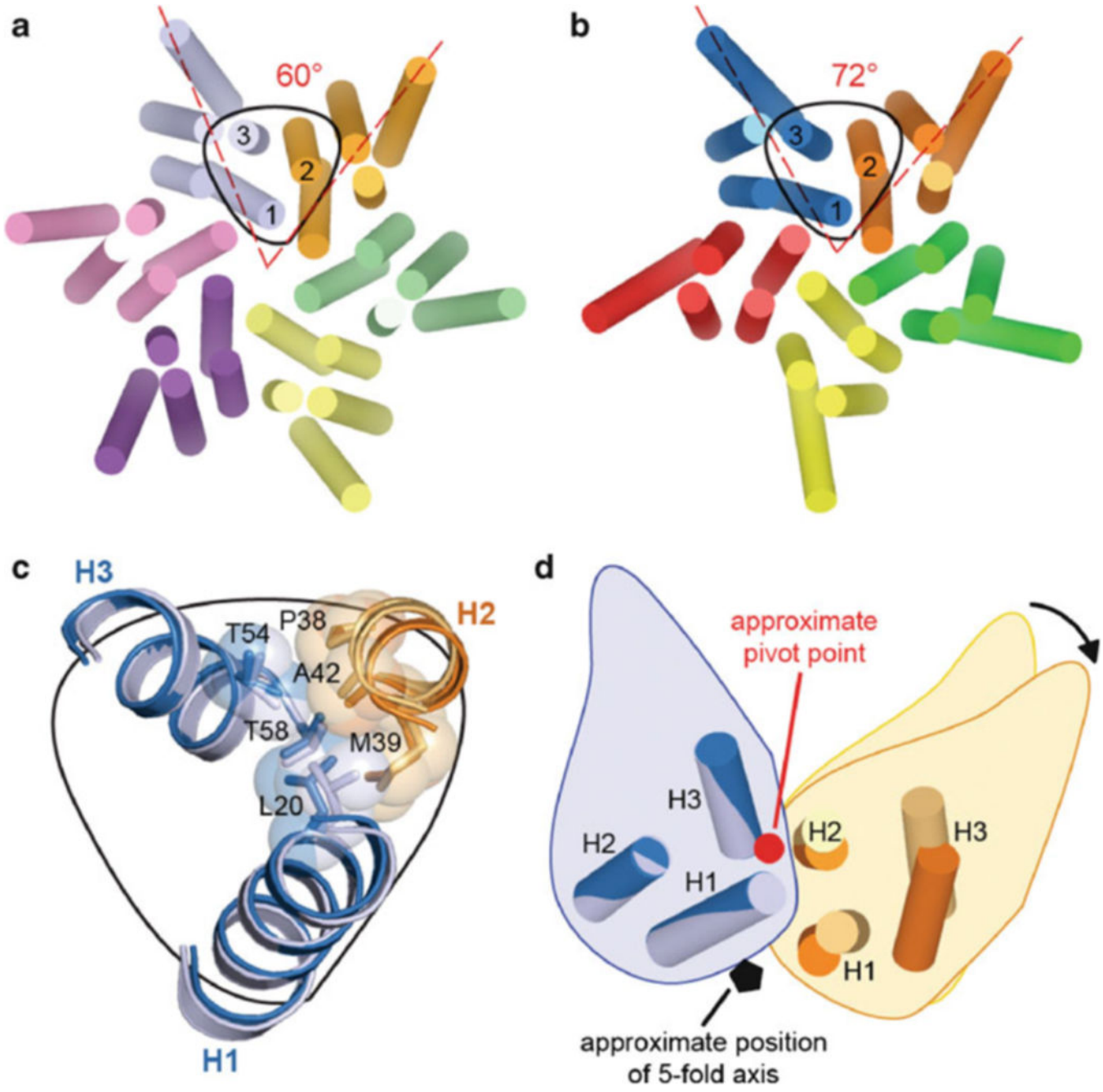

Fig. 10.

Quasi-equivalence in the pentameric and hexameric CA^{NTD} rings. Top views of the (**a**) hexameric and (**b**) pentameric CA^{NTD} rings, with each subunit in a different color. Subunits in the pentamer and hexamer are shown in *darker* and *lighter* shades, respectively. The angles subtended by adjacent domains are shown explicitly for the *blue* and *orange* subunits. One of the repeating three-helix units is outlined in *black*. (**c**) Close-up view of the pentameric and hexameric repeat units, superimposed on helices 1 and 3 of the *blue* subunit. The aliphatic residues that form a small hydrophobic core are shown explicitly and labeled. (**d**) The "rotation" between adjacent subunits, in going from the hexamer to the pentamer.

The approximate position of the rotation axis is indicated by the *red dot*. Note that this axis is parallel to neither the pentameric nor hexameric symmetry axes. (Reprinted from Pornillos et al. (2011), with permission from Macmillan Publishers Ltd.)

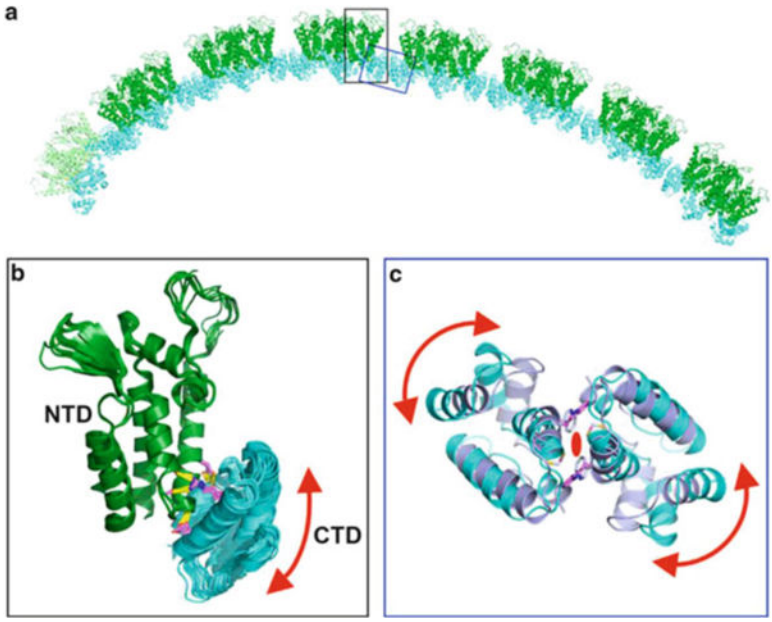

Fig. 11.

Proposed mechanisms for generating curvature in the mature retroviral capsid. (**a**) Structural model of the capsid, showing a line of connected rings. The CA^{NTD} hexamers are colored in *green*, and CA^{CTD} dimers are in *cyan*. One pentamer is shown on the *left*, with the CA^{NTD} colored *light green*. The two regions that are proposed to contribute to curvature generation are indicated by the *black box* (NTD–CTD interface) and the *blue box* (CTD–CTD dimer interface). (**b**) Flexion at the intermolecular NTD–CTD interface occurs about molecular pivots composed of helix-capping hydrogen bonds. Shown are 17 independent X-ray structures of the NTD–CTD interface, superimposed on the CA^{NTD} domain. Rigid-body movement of CA^{CTD} relative to CA^{NTD} is indicated by the *red double-headed arrow*. Hydrogen-bonded side chains are shown explicitly. Hydrogen bonds are indicated as *yellow lines*. (**c**) Superposition of the X-ray structure (colored *light blue*) (Worthylake et al. 1999) and NMR structure (colored *cyan*) (Byeon et al. 2009) of the isolated full-affinity CA^{CTD} dimer. The structures show distinct configurations of the dimer. The *red double-headed arrows* indicate putative slippage or rotation about the dimer symmetry axis (*red oval*).